

# **GNSS Multipath Analysis and Processing Software (MAPS) User Manual**

Written by Zhetao Zhang ([zt.zhang@hotmail.com](mailto:zt.zhang@hotmail.com)),  
Jingjing Yang, and Haijun Yuan ([navyyuan@yeah.net](mailto:navyyuan@yeah.net))



**Research group of GNSS+ under  
Complex Conditions (GCC)**

Dec 2024

## Contents

1 Introduction.....	1
2 Mathematical model.....	1
2.1 Multipath analysis model.....	1
2.1.1 CMC method.....	1
2.1.2 GFix and IC method.....	1
2.1.3 GF and IC method.....	2
2.1.4 C/N0 template function.....	3
2.2 MHM model.....	4
2.2.1 Unified and differentiated MHM .....	4
2.2.2 MHM precision model.....	5
2.2.3 MHM refined by trend surface analysis.....	6
2.3 SF model.....	7
2.3.1 Traditional SF model.....	7
2.3.2 Window-matching SF model .....	7
3 Architecture of the MAPS.....	8
3.1 Module and function .....	8
3.2 Directory structure .....	9
4 How to Run the MAPS .....	13
4.1 MATLAB version .....	13
4.2 Input data .....	14
4.3 Multipath analysis.....	14
4.4 MHM modeling .....	16
4.5 SF modeling.....	18
5 Plotting function.....	20
5.1 Plotting of multipath analysis .....	20
5.1.1 CMC method.....	20
5.1.2 GFix and IC method.....	23
5.1.3 GF and IC method.....	23
5.1.4 C/N0 template function.....	24
5.2 Plotting of MHM modeling .....	24
5.2.1 2D sky plot.....	24
5.2.2 2D plane plot.....	27
5.2.3 3D sky plot.....	30
5.3 Plotting of SF modeling.....	31
6 Acknowledgement.....	33
7 Disclaimer.....	34
8 Contact us.....	34
Reference .....	34

# 1 Introduction

As one of the main error sources in Global Navigation Satellite Systems (GNSS) precise data processing, multipath effects are necessary to be analyzed and processed. An open-sourced GNSS multipath analysis and processing software (MAPS) is introduced and developed based on MATLAB 2021a. This user manual introduces the MAPS in detail, which is a multipath analysis and processing software for the multi-constellation and multiple-frequency GNSS observations including GPS, GLONASS, Galileo, and BDS. Using this software, one can easily analyze the multipath and build the corresponding models to process the multipath, such as multipath hemispherical map (MHM) models and sidereal filter (SF) models. Additionally, the MAPS also provides the diversity of plotting types to show the corresponding modeling results.

## 2 Mathematical model

### 2.1 Multipath analysis model

#### 2.1.1 CMC method

The most widely used method for assessing the multipath effects is the code multipath combination (CMC) method ([Zhang et al. 2021](#)). This method requires at least two frequencies of phase observations, which can be expressed as ([Leick et al. 2015](#))

$$\bar{M}_{r,i}^{ks} = P_{r,i}^s - \frac{f_i^2 + f_j^2}{f_i^2 - f_j^2} \phi_{r,i}^{ks} + \frac{2f_j^2}{f_i^2 - f_j^2} \phi_{r,j}^{ks} + \frac{f_i^2 + f_j^2}{f_i^2 - f_j^2} \lambda_i N_i - \frac{2f_j^2}{f_i^2 - f_j^2} \lambda_j N_j - \xi_{r,i} + \xi^{s,i} + \epsilon_{\bar{M}_{r,i}^{ks}} \quad (1)$$

where  $s$  and  $r$  denote the satellite and receiver, respectively.  $i$  and  $j$  denote the corresponding frequencies,  $P$  and  $\phi$  denote the code and phase observations, respectively.  $\lambda$  and  $N$  denote the wavelength and ambiguity, respectively.  $\xi$  and  $\epsilon$  denote the code hardware delay and observation noise, respectively.  $\bar{M}$  denotes the equivalent code multipath consisting of the ambiguities of two frequencies, and receiver and satellite code hardware delays. Without cycle slips, the above error terms can be regarded as a constant during a certain period. Hence, the code multipath can be obtained as

$$M_{r,i}^s = \bar{M}_{r,i}^s - \frac{1}{n} \sum_{t=1}^n [\bar{M}_{r,i}^s(t)] \quad (2)$$

where  $n$  denotes the epoch number. The CMC method is widely used due to its high reliability. However, there are mainly two limitations. First, only the peak-to-peak behaviors of the code multipath can be estimated. Second, it can only work when there are two or more frequencies for a certain constellation.

#### 2.1.2 GFix and IC method

In the geometry-fixed (GFix) and ionospheric-corrected (IC) method ([Zhang et al.](#)

2021), the observations need to be preprocessed. Specifically, the satellite clock errors should be corrected based on the broadcast or precise ephemeris. After the atmospheric delays are corrected, the code and phase observation equations can be deduced as

$$P_{r,i}^s = \rho_r^s + \delta t_r + \xi_{r,i} + M_{r,i}^s + \epsilon_{r,i}^s \quad (3)$$

$$\phi_{r,i}^s = \rho_r^s + \lambda_i N_{r,i}^s + \delta t_r + \zeta_{r,i} - \zeta^{s,i} + \xi^{s,i} + m_{r,i}^s + \varepsilon_{r,i}^s \quad (4)$$

where  $\delta t_r$  and  $\zeta$  denote the receiver clock error and phase hardware delay, respectively. Since the receiver clock error and hardware delay need to be eliminated, the between-satellite single differencing is formed as

$$P_{r,i}^{ks} = \rho_r^{ks} + M_{r,i}^{ks} + \epsilon_{r,i}^{ks} \quad (5)$$

$$\phi_{r,i}^{ks} = \rho_r^{ks} + \lambda_i N_{r,i}^{ks} - \zeta^{ks,i} + \xi^{ks,i} + m_{r,i}^{ks} + \varepsilon_{r,i}^{ks} \quad (6)$$

Based on the precise coordinates of the test station and satellites used, the GFix model is applied. When estimating the satellite coordinates, the broadcast or precise ephemeris can be used according to the demands of the users. Hence, the code multipath can be estimated as

$$E[M_{r,i}^{ks}] = P_{r,i}^{ks} - \rho_r^{ks} \quad (7)$$

where “ $E[\cdot]$ ” denotes the expectation operator. For the phase multipath, the bias term  $b = \lambda_i N_{r,i}^{ks} - \zeta^{ks,i} + \xi^{ks,i}$  can be treated as a constant when there are no cycle slips.

Hence, the bias term can be removed by averaging over a certain period. Then, the phase multipath effects are estimated as

$$E[m_{r,i}^{ks}] = \phi_{r,i}^{ks} - \rho_r^{ks} - b \quad (8)$$

with  $b = \frac{1}{n} \sum_{t=1}^n [\phi_{r,i}^{ks}(t) - \rho_r^{ks}(t)]$ . The biggest advantage of the GFix and IC method is that it can still work even if there is only one observable satellite in addition to the reference satellite. However, its accuracy is highly dependent on the precision of the coordinates of the test station and used satellites. As usual, the accuracies of orbit and satellite clock are approximately 100 cm and 5 ns when using the broadcast ephemeris. However, for the precise ephemeris, these values can reach approximately 2.5 cm and 75 ps. Hence, it is better to apply the precise ephemeris. Besides, the multipath effects of the reference satellite are also included in the GFix and IC method.

### 2.1.3 GF and IC method

For the geometry-free (GF) and IC method (Zhang et al. 2021), the preprocessing is like that of the GFix and IC method. After preprocessing, the time-differenced operator is used. Then, the hardware delays and phase ambiguities can be regarded as eliminated

in case of no cycle slips. The corresponding code and phase observations are deduced as

$$\Delta P_{r,i}^s = \Delta \rho_r^s + \Delta \delta t_r + \Delta M_{r,i}^s + \Delta \epsilon_{r,i}^s \quad (9)$$

$$\Delta \phi_{r,i}^s = \Delta \rho_r^s + \Delta \delta t_r + \Delta m_{r,i}^s + \Delta \varepsilon_{r,i}^s \quad (10)$$

where “ $\Delta$ ” denotes the time-differenced operator. Since the above observation models are rank deficient, the parameters need to be combined as

$$\Delta P_{r,i}^s = \Delta \tilde{\rho}_r^s + \Delta M_{r,i}^s + \Delta \epsilon_{r,i}^s \quad (11)$$

$$\Delta \phi_{r,i}^s = \Delta \tilde{\rho}_r^s + \Delta \tilde{\varepsilon}_{r,i}^s \quad (12)$$

with  $\Delta \tilde{\rho}_r^s = \Delta \rho_r^s + \Delta \delta t_r$ ,  $\Delta \tilde{\varepsilon}_{r,i}^s = \Delta m_{r,i}^s + \Delta \varepsilon_{r,i}^s$ . Then, the time-differenced code multipath effects can be estimated as

$$E[\Delta M_{r,i}^s] = \Delta P_{r,i}^s - \Delta \phi_{r,i}^s \quad (13)$$

This method is also convenient and can work under any conditions, but the method also has some limitations. First, only the time-differenced code multipath effects can be depicted, where the undifferenced multipath is missing. Second, the phase multipath effects cannot be obtained.

#### 2.1.4 C/N0 template function

The modeling procedure of the carrier-to-noise density ratio (C/N0) template function mainly includes the following four steps ([Strode and Groves 2015](#); [Zhang et al. 2019](#)). The first step is the consistency checking. Since the C/N0 is influenced by the power output of the satellite transmitter, one needs to check whether the observed C/N0 from different satellites are significantly discrepant. Since the C/N0 template observations can be treated to be normally distributed, a threshold of 3-sigma is applied ([Koch 1999](#)). Specifically, the observed C/N0 of one certain satellite  $s$  should be classified if

$$|\overline{C/N0}_s - \overline{C/N0}| \geq 3\sigma_{C/N0} \quad (14)$$

where  $\overline{C/N0}_s$  denotes the mean value of C/N0 for the certain satellite  $s$ ;  $\overline{C/N0}$  denotes the mean value of C/N0 for all the satellites classified in the same group;  $\sigma_{C/N0}$  denotes the corresponding standard deviation (STD).

The second step is to check the minimum sample size of C/N0 template observations. It is noted that if the number of template dataset is too few, the accuracy of the C/N0 template function is limited. Because the C/N0 template observations are independent and normally distributed in each elevation interval (e.g., 0.1 degrees), the minimum sample size  $n_{min}$  can be estimated as ([Lehmann and Romano 2006](#))

$$n_{min} \geq Z_{1-\alpha/2}^2 \frac{\sigma^2}{\varepsilon^2} \quad (15)$$

where  $Z_{1-\alpha/2}$  denotes the quantile of standard normal distribution with a significance level of  $\alpha$ ;  $\sigma$  and  $\varepsilon$  denote the STD and absolute error, respectively. In general, we

can assume that  $\alpha = 0.05$  (i.e.,  $Z_{1-\alpha/2} = 1.96$ ) and  $\sigma = 3\varepsilon$ , thus causing  $n_{\min} = 35$  for each 0.1-degree interval. Hence, we apply  $n_{\min} = 350$  for each 1-degree elevation interval.

Then, if the number of C/N0 observations is larger than the  $n_{\min}$  in each elevation interval, the raw template dataset can be refined. Specifically, the C/N0 observations will be deleted if their values exceed three or two times of their STDs in each elevation interval. This step is iterative until the appropriate threshold is determined as

$$\forall \theta, \exists n(\kappa\alpha) \geq n_{\min} \quad (16)$$

where  $\kappa$  denotes the threshold to be determined;  $n(\kappa\alpha)$  denotes the numbers of C/N0 within  $\kappa\alpha$ .

Finally, the C/N0 template observations and the corresponding STDs can be fit using the elevation-dependent functions (e.g., the third-order polynomials). It is worth noting that these template functions usually only need to be determined once in advance unless the signal strength is changed by the official government.

## 2.2 MHM model

### 2.2.1 Unified and differentiated MHM

For MHM modeling, the double-differenced (DD) residuals, single-differenced (SD) residuals, and un-differenced (UD) residuals can be used (Zhang et al. 2023). However, since the MHM is established according to one satellite, it is recommended to conduct the transformation of residuals. That is, one needs to convert the DD residuals into SD residuals between the receivers by

$$\begin{bmatrix} \hat{\mathbf{P}}_{\text{DD}} \\ \hat{\boldsymbol{\Phi}}_{\text{DD}} \end{bmatrix} = \mathbf{B} \cdot \begin{bmatrix} \hat{\mathbf{P}}_{\text{SD}} \\ \hat{\boldsymbol{\Phi}}_{\text{SD}} \end{bmatrix} \quad (17)$$

where  $\hat{\mathbf{P}}_{\text{SD}}$  and  $\hat{\boldsymbol{\Phi}}_{\text{SD}}$  denote the code and phase SD residual samples, respectively. Due to the rank deficient of design matrix  $\mathbf{B}$  caused by the existence of the reference satellite, one cannot directly obtain the SD residual samples based on Eq. (17). Hence, the implementation of an additional constraint is required, albeit with the possibility of introducing additional bias. In this study, a commonly used zero-mean constraint based on elevation was adopted as

$$\begin{cases} \sum_{i=1}^s \varpi \hat{\mathbf{P}}_{\text{DD}}^i = 0 \\ \sum_{i=1}^s \varpi \hat{\boldsymbol{\Phi}}_{\text{DD}}^i = 0 \end{cases} \quad (18)$$

where  $\hat{\mathbf{P}}_{\text{DD}}^i$  and  $\hat{\boldsymbol{\Phi}}_{\text{DD}}^i$  denote the  $i$ -th DD samples of  $\hat{\mathbf{P}}_{\text{DD}}$  and  $\hat{\boldsymbol{\Phi}}_{\text{DD}}$ , respectively.  $\varpi$  denotes the elevation-dependent weighting scheme. It is worth noting that the zero-mean assumption in MHM is not completely strict because the difference in satellite constellation distribution may affect the zero-mean reference. To address this issue, more strict strategies can be employed, such as incorporating random walk constraints or multi-point hemispherical grids. However, for practical reasons, a quality control

strategy is widely adopted. Specifically, only the satellites with a certain high elevation (e.g.,  $\beta$ ) are selected as reference satellites in the acquisition of DD samples, thereby minimizing the potential bias associated with the zero-mean assumption.

The modeling procedure of traditional MHM model is mainly divided into three steps, which are as follows:

- (1) According to the satellite azimuth and elevation and the desired grid resolution, the residuals are divided into different grids.
- (2) Quality control strategies are conducted in each grid to eliminate the outliers of residual samples. Assuming the residuals are normally distributed, the samples that exceed twice the STD are excluded. Besides, only when the number of remaining samples is greater than a certain value, the estimated multipath correction in this grid is regarded as valid. In this study, the minimum sample size  $num_{min}$  can be determined as

$$num_{min} \geq Z_{1-\alpha/2}^2 \left( \frac{STD}{E} \right)^2 \quad (19)$$

where  $STD$  denotes the standard deviation of absolute error  $E$ . The absolute error  $E$  denotes the difference between the multipath correction and the corresponding reference value in this grid. Without loss of generality, the value of  $\alpha$  is set to 5%, and the ratio between  $STD$  and  $E$  is set to 2. Consequently,  $num_{min}$  in each grid is 16 in this study.

- (3) Finally, according to the mean values of remaining residual samples in each grid, high-precision and high-reliability MHM can be modeled according to a specific criterion. That is, one can construct a unified MHM model regardless of the observation type. Also, differentiated MHM models can be established according to the orbit and frequency types of satellites (i.e., SMHM and FMHM) ([Zhang et al. 2023](#)).

### 2.2.2 MHM precision model

For the MHM precision (PMHM) model ([Zhang et al. 2024](#)), the mean standard deviation (MSTD) is adopted as the grid value. In multipath modeling, the mean value of residuals in each grid is regarded as the multipath correction of this grid. Because all residual samples contain errors, the mean value will also contain errors. The MSTD can express the accuracy of the mean value of a sample set. The traditional STD reflects the degree of dispersion for a sample set in a grid. While the MSTD reflects the reliability of the obtained mean value of this grid. Here, the mean value of samples is applied as the multipath correction. Therefore, compared to the traditional STD, the MSTD can better reveal whether the multipath correction is reliable.

The MSTD  $S$  for a certain elevation and azimuth grid in the MHM precision model can be defined as

$$S = \sqrt{\frac{\sum_{i=1}^n (y_i - \bar{y})^2}{n-1}} \quad (20)$$

where  $\bar{y}$  denotes the mean value of a certain grid in the MHM model (i.e., multipath correction);  $y_i$  denotes the multipath correction sample of index  $i(i = 1, 2, \dots, n)$  with  $n$  denoting the number of multipath correction samples in the grid.

### 2.2.3 MHM refined by trend surface analysis

For the MHM refined by trend surface analysis (T-MHM) ([Wang et al. 2019; Lu et al. 2021; Yuan et al. 2024](#)), the station sky is divided into azimuth and elevation grids. Then, T-MHM performs trend surface analysis to fit the multipath variations inside each grid, which can be expressed as

$$m_i(a_i, e_i) = \hat{m}_i(a_i, e_i) + \epsilon_i \quad (21)$$

where  $i = 1, 2, \dots, n$  denotes the sample index in a certain grid.  $(a_i, e_i)$  denote the coordinates of the residual sample in the grid determined by the azimuth and elevation.  $m_i$  and  $\hat{m}_i$  denote the multipath observations and multipath estimates, respectively.  $\epsilon_i$  denotes the unfitted residual within the grid.

The mathematical equations used to calculate the trend surface include polynomial functions and Fourier series. Usually, T-MHM utilizes the commonly used polynomial functions, which are expressed as

$$\hat{m}_i(a_i, e_i) = b_0 + b_1 a_i + b_2 e_i \quad (22)$$

where  $b_0$ ,  $b_1$ , and  $b_2$  denote the polynomial coefficients. Let  $a_i = N_{1i}$ ,  $e_i = N_{2i}$ . The general formula of the trend surface can be written as

$$\hat{m}_i = b_0 + b_1 N_{1i} + b_2 N_{2i} \quad (23)$$

Then, the least squares normal equations can be expressed as

$$(N^T N)B = N^T M \quad (24)$$

where  $N = \begin{bmatrix} 1 & N_{11} & N_{21} \\ 1 & N_{12} & N_{22} \\ \vdots & \vdots & \vdots \\ 1 & N_{1n} & N_{2n} \end{bmatrix}$ ,  $M = \begin{bmatrix} m_1 \\ m_2 \\ \vdots \\ m_n \end{bmatrix}$  and  $B = \begin{bmatrix} b_0 \\ b_1 \\ b_2 \end{bmatrix}$ . Then, the polynomial

coefficients of the trend surface can be estimated as

$$\hat{B} = (N^T N)^{-1} N^T M \quad (25)$$

It is noted that the linear, quadratic, and cubic trend surfaces can be reasonably choose in practical applications. To avoid under-fitting and over-fitting of multipath variation within grids, some statistic criteria can be utilized, such as the goodness-of-fit test and significance test ([Sobol 1991; Cornell 1987; Anscombe 1973](#)). When the statistical tests are failed, the mean value of residuals can be adopted as the multipath correction in this grid.

## 2.3 SF model

### 2.3.1 Traditional SF model

The modeling procedure of traditional SF model is mainly divided into the following three steps ([Bock et al. 2000](#)):

- (1) According to the daily broadcast ephemeris, the satellite orbit repetition period is calculated at each epoch. The formula for calculating the satellite orbit repetition period using Kepler's third law is

$$t_s = \frac{2k\pi}{\sqrt{GM}a^{-\frac{3}{2}} + \Delta n} \quad (26)$$

where  $t_s$  denotes the satellite orbit repetition period.  $k$  denotes the number of satellite revolutions.  $\sqrt{GM}$  denotes the standard gravity parameter.  $a$  denotes the semi-major axis of satellite orbit.  $\Delta n$  denotes the correction for the satellite angular velocity.

- (2) Allocate the residuals for different satellites at each epoch and conduct the wavelet filtering on the residuals at each epoch to mitigate the noise.
- (3) Finally, the advanced satellite period at the current epoch is obtained by using the broadcast ephemeris. Then, the corresponding residual of a cycle of the satellite is used as a correction to correct the multipath at the current epoch. That is, a model for real-time multipath correction of each satellite can be constructed based on the residuals of different satellites at different epochs.

### 2.3.2 Window-matching SF model

For the traditional SF model, the core is to find the satellite orbital period based on the broadcast ephemeris. Then, the window-matching SF (abbreviated as SF\_W) model is proposed based on the correlation of residuals. The modeling procedure of SF\_W model is mainly divided into the following three steps:

- (1) According to the obtained residuals, it is necessary to first determine the number of epochs contained in each window, i.e., the size of the window.
- (2) Then, a cross-correlation method (CCM) is used to find the window with the highest correlation coefficient between the current window and the window in the residuals obtained in advance. The CCM is a common method to obtain multipath repeat time ([Ragheb et al. 2007](#)), which determines the repeat time according to the correlation coefficient after staggering the different epochs between two residual series. The correlation coefficient is defined as

$$\rho_{XY} = \frac{\text{Cov}(X,Y)}{\sqrt{D(X)}\sqrt{D(Y)}} \quad (27)$$

$$\text{Cov}(X, Y) = \frac{1}{n} \sum_n^1 (x_i - \mu_x)(y_j - \mu_y) \quad (28)$$

where  $X$  denotes the current residual series and  $Y$  denotes the obtained residual

series in advance with the same size as  $X$ .  $Cov(X, Y)$  denotes the covariance of  $X$  and  $Y$ .  $D(X)$  and  $D(Y)$  denote the variance of  $X$  and  $Y$ , respectively. When the value of  $\rho_{XY}$  is the maximum, the staggered epoch is the sidereal shift.

- (3) According to the residual series of the two best matching windows, a multipath solution based on least squares is performed. Specifically, the satellite SD residuals are divided into the certain segments such as segment I and segment II. At the same time, segment II overlaps with the previous segment I to ensure a near real-time performance. The CCM is used to calculate the multipath repeat time of different segments. Then, for the  $i$ -th epoch on current residual series, the template window is formed by several epochs as

$$x_2(t_{i-l}), \dots, x_2(t_{i-1}), x_2(t_i), x_2(t_{i+1}), \dots, x_2(t_{i+l}) \quad (29)$$

where  $i$  denotes the epoch index and the window size is the number of epochs. The matched window is determined by the repeat time obtained by the CCM.

- (4) Assuming that both the template window and matched window have been obtained, the following affine transformation model ([Shen et al. 2020](#)) is applied to determine the value of multipath correction of the  $i$ -th epoch as

$$\begin{bmatrix} x_2(t-l) \\ \vdots \\ x_2(t) \\ \vdots \\ x_2(t+l) \end{bmatrix} = \begin{bmatrix} x_1(t-l) & 1 \\ \vdots & \vdots \\ x_1(t) & 1 \\ \vdots & \vdots \\ x_1(t+l) & 1 \end{bmatrix} \begin{bmatrix} a \\ b \end{bmatrix} + \varepsilon \quad (30)$$

where  $a$  and  $b$  denote the scaling factor and translation factor, respectively.  $\varepsilon$  denotes the random noise. The parameters  $a$  and  $b$  can be estimated by the least square method. The weight matrix is determined according to the distance between the epochs. The closer to the  $i$ -th epoch, the greater the weight of sample.

In conclusion, the SF\_W model can construct a real-time multipath correction for each satellite based on the residuals of different satellites at different epochs, which is also superior to the traditional SF model in terms of stability.

### 3 Architecture of the MAPS

#### 3.1 Module and function

The MAPS integrates two core modules including the multipath analysis module and multipath processing module, and the flowchart of MAPS is shown in Fig. 1.

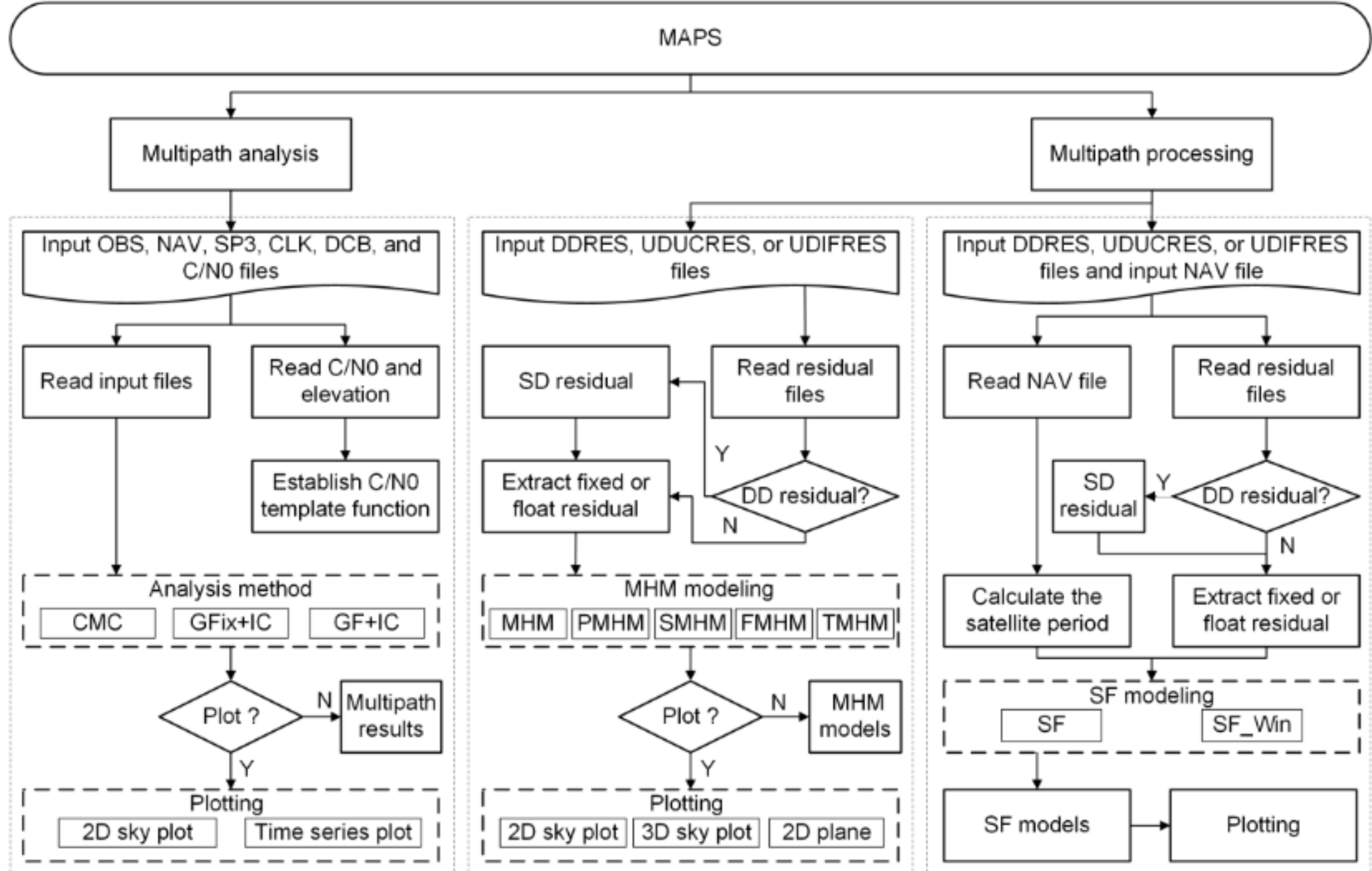


**Fig. 1** Flowchart of the MAPS

Specifically, the multipath analysis module includes three multipath estimation methods: the CMC method, the GFix and IC method, and the GF and IC method. The above methods can accurately estimate and analyze the multipath even in the challenging environments, which is beneficial to GNSS multipath processing and the improvement of accuracy and reliability of PNT applications. The results of estimated multipath can also be plotted, and the plotting types include time series plot and sky plot. In addition, the multipath analysis module supports the establishment of C/N0 template function, which is important to accurately depict and detect the multipath in the challenging environments. In this part, the “XXX.ddres” file will be read, which contains the elevation and C/N0 values of satellites. Then, the C/N0 template function modeling and plotting are carried out.

In the multipath processing module, five types of MHM models are supported including the traditional MHM, PMHM, SMHM, FMHM, and TMHM models. For these models, it is necessary to read the residual files. There are three types of residual forms used in MHM modeling, including double differenced residual (DDRES), undifferenced and ionospheric-free residual (UDIFRES), and undifferenced and uncombined residual (UDUCRES). In addition, two types of SF models are supported in the multipath processing module including the traditional SF model and the window matching SF (SF\_W) model. In conclusion, the MAPS can efficiently analyze and process the multipath for multiple GNSS systems, laying a solid foundation for realizing high-precision GNSS PNT applications.

### 3.2 Directory structure

As shown in Fig. 2, there are eight folders and three scripts in the MAPS. The script named “main\_MPAnalysis.m” includes three multipath estimation methods and the modeling of C/N0 template function in the multipath analysis module. The two scripts

named “main\_MHMModel.m” and “main\_SFModel.m” are the MHM modeling and SF modeling in the multipath processing module. At the same time, there are 8 folders. Specifically, **0\_Input** folder includes the input datasets; **1\_Read** folder includes the reading functions; **2\_Preprocess** folder includes the preprocessing functions; **3\_MPAnalysis** folder includes the functions of analyzing multipath; **4\_MHMmodel** and **5\_SFmodel** folders include the functions of MHM modeling and SF modeling of processing multipath, respectively; **6\_Plot** folder includes the functions for plotting; **7\_Output** folder includes the output datasets; **8\_Tool** folder includes the other common functions.

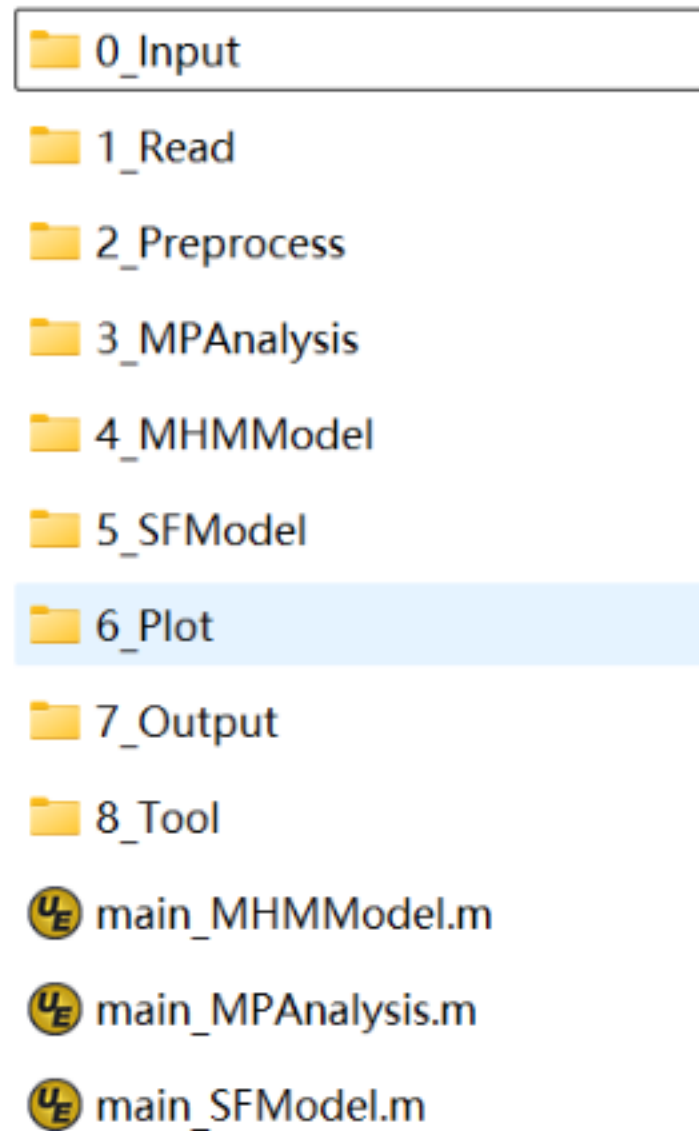


**Fig. 2** Directory structure of the MAPS

Given the variability of the input data, the following discussion will focus on the relevant contents within the **0\_Input** folder. Specifically, **0\_Input** folder includes the data files needed in the MAPS. As shown in Fig. 3, in the multipath analysis module, the observation file, precise ephemeris file, precise clock file, broadcast ephemeris file, DCB file, ATX file, and C/N0 file are needed. Since the data files required for multipath processing module (i.e., the MHM and SF modeling) are similar, the data files required for the two modules is put together in this folder. Several different types of residual files and broadcast ephemeris files are used in the MAPS, where the sources of the used raw files are summarized in Table 1.

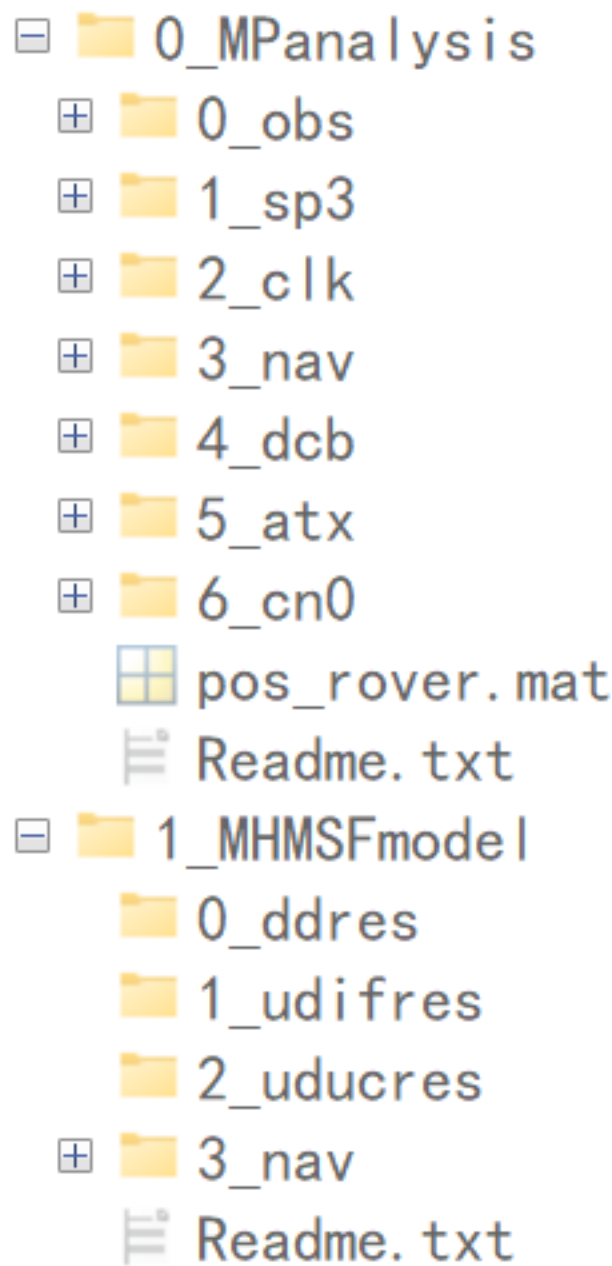


**Fig. 3** Directory structure of the ‘0\_Input’ folder

**Table 1** Sources of the used raw files

Files type	Example	Source
Precise ephemeris	WUM0MGXFIN_2024070000_01D_05M_ORB.SP3	ftp://igs.gnsswhu.cn/pub/gnss/products/mgex/
Precise clock	WUM0MGXFIN_2024070000_01D_30S_CLK.CLK	
Broadcast ephemeris	BRDM00DLR_S_2024070000_01D_MN.rnx	ftp://igs.gnsswhu.cn/pub/gps/data/daily/
DCB	CAS0MGXRAP_2024070000_01D_01D_DC.BSX	https://data.bdsmart.cn/pub/product/bias/
ATX	igs.atx	https://files.igs.org/pub/staton/general/
DD residual	2024007.ddres	
UDIF residual	2024007.udifres	Calculated from the RTKLIB software
UDUC residual	2024007.uducres	
Observation	2024007.obs	Self-observed

As shown in Table 1, it is noted that the DDRES, UDIFRES, and UDUCRES files can be calculated by the RTKLIB software and can be found in the github website ([https://github.com/GCCProTeam/MAPS\\_ResidualDatasets](https://github.com/GCCProTeam/MAPS_ResidualDatasets)). Table 2 lists the satellite periods of GPS, GLONASS, Galileo, and BDS. Since the longest satellite period is approximately 10 sidereal days, the 10-day residuals are prepared here. In addition, it is worth noting the specific encoding formats of the residual files used in the MAPS. When preparing these residual files, it is necessary to ensure the consistency and correctness of the file formats, which is related to the subsequent processing of reading residual files. Examples of three types of the residual file formats are given below. Figs. 4 to 6 show the examples of DDRES, UDICRES, and UDUCRES files, respectively. Among Figs. 4 to 6, the data within the red solid frame is the satellite azimuth and elevation, and that within the green solid frame is the satellite fixed mark, phase residual, code residual, and C/N0 value. The data within the different green solid frames denote

the results of different frequencies for satellites. For UDIFRES file, there is only one frequency because of using the IF model.

**Table 2** Satellite periods of GPS, GLONASS, Galileo, and BDS

System	Orbit type	Period (sidereal day)
GPS	MEO	≈1
GLONASS	MEO	≈8
Galileo	MEO	≈10
	GEO	≈1
BDS	IGSO	≈1
	MEO	≈7

2024007.ddres											
1	\$GPST	2295	684800	1							
2	G10	311.7356	70.4269	1	0.0000	0.0000	50.9	1	0.0000	0.0000	50.0
3	G12	93.5916	41.8635	1	0.0014	-0.2553	46.8				
4	G15	95.4434	11.5814	1	-0.0035	-0.5344	39.1				
5	G18	191.7667	10.8688	1	-0.0107	0.1879	45.4	1	0.0036	-0.6201	44.3
6	G23	153.2999	66.3348	1	-0.0022	0.3207	50.2	1	0.0062	-0.1123	50.1
7	G24	47.3302	24.0952	1	-0.0003	0.2683	40.8	1	0.0057	0.1083	44.6
8	G25	145.1826	43.8448	1	-0.0012	-0.5038	46.2	1	0.0015	-0.2778	46.5
9	G28	239.0651	27.8186	1	-0.0013	-0.6025	47.6	1	0.0011	-0.0875	44.7
10	G32	311.0185	41.8931	1	0.0038	-0.4639	47.9	1	-0.0014	-0.0999	45.9
11	R01	95.7902	32.9276	1	0.0021	-0.1301	46.3	1	-0.0059	-0.7621	42.4
12	R02	20.2384	55.6456	1	0.0008	-0.4263	52.8	1	0.0004	-0.8513	50.3
13	R03	321.8987	22.5926	1	-0.0025	0.1311	46.4	1	-0.0005	-0.6229	47.5
14	R11	29.1169	14.0437	1	0.0027	0.0508	42.8	1	0.0026	-0.0502	42.5
15	R12	66.0646	67.8161	1	0.0000	0.0000	52.6	1	0.0000	0.0000	50.8
16	R13	183.3851	51.1409	1	-0.0047	-1.5333	42.9	1	-0.0047	0.2827	41.4
17	R18	288.1601	12.4692	1	0.0030	-0.7454	42.2	1	0.0043	-1.0024	43.1
18	C01	137.5061	43.5947	1	-0.0006	0.9164	43.0	1	-0.0041	0.0444	42.3
19	C02	234.7230	38.9551	1	0.0051	1.4552	39.4	1	0.0039	0.2932	40.9
20	C03	195.8611	52.6295	1	0.0028	0.4828	42.7	1	0.0014	0.0838	43.7
21	C04	121.5219	31.9011	1	-0.0008	1.3234	39.4	1	0.0023	0.2114	39.9
22	C05	255.0025	17.8556								
23	C06	282.3063	65.6286	1	-0.0002	0.9236	45.1	1	0.0004	0.0746	44.9
24	C13	236.7851	73.3346	1	0.0022	1.1977	47.6	1	-0.0016	-0.1703	47.1
25	C16	285.5252	65.6834	1	0.0011	1.4113	47.6	1	0.0005	0.0073	43.6
26	C21	330.0090	53.6727	1	0.0039	0.7655	49.8	1	0.0003	-0.1065	49.3
27	C22	91.4676	68.5122	1	0.0019	0.6938	50.2	1	0.0026	-0.0112	49.9
28	C26	210.0717	27.3359	1	0.0052	0.5504	44.1	1	-0.0028	0.0464	44.0
29	C36	46.6883	36.2718	1	0.0047	1.1684	46.3	1	-0.0007	0.0814	47.2
30	C38	180.2635	56.9982	1	0.0010	0.4431	47.4	1	0.0022	0.1571	47.0
31	C39	316.5048	69.4724	1	0.0026	0.3915	48.2	1	0.0018	-0.0745	49.3
32	C45	146.7652	76.9709	1	0.0000	0.0000	49.2	1	0.0000	0.0000	50.9
33	C59	142.4585	47.6479	1	0.0005	0.8779	45.2	1	0.0017	-0.1511	46.8

**Fig. 4** Example of DDRES file

2024007.udifres						
0	1.0	2.0	3.0	4.0	T	5.0
1	\$GPST	2296	000000	6		
2	G10	311.7356	70.4269	1	0.0013	0.2704 50.9
3	G12	93.5916	41.8635	1	0.0018	-0.7410 46.8
4	G15	95.4434	11.5814	1	0.0058	-1.0188 39.1
5	G18	191.7667	10.8688	1	0.0061	1.2885 45.4
6	G21	316.3169	5.5540	1	0.0109	2.3548 39.2
7	G23	153.2999	66.3348	1	0.0013	-0.4830 50.2
8	G24	47.3302	24.0952	1	0.0029	0.2553 40.8
9	G25	145.1026	43.0441	1	0.0018	0.0722 46.2
10	G28	239.0651	27.8180	1	0.0025	0.3236 47.0
11	G31	231.9086	3.5013	1	0.0153	-3.4631 37.8
12	G32	311.0185	41.8931	1	0.0018	0.6161 47.9
13	R01	95.7902	32.9276	1	0.0022	0.4232 43.9
14	R02	20.2384	55.6450	1	0.0015	-1.2074 51.2
15	R03	321.8987	22.5926	1	0.0031	-2.0498 44.5
16	R11	29.1169	14.0437	1	0.0048	2.1932 40.5
17	R12	66.0646	67.8161	1	0.0013	0.3822 51.0
18	R13	183.3851	51.1409	1	0.0015	0.7967 41.3
19	R17	242.6850	7.2759	1	0.0087	-0.5399 41.8
20	R18	288.1601	12.4692	1	0.0054	2.1666 41.2
21	R19	327.9801	4.8559	1	0.0121	-4.0278 32.3
22	E04	73.4307	34.6619	1	0.0021	0.8695 46.9
23	E05	295.9226	25.2773	1	0.0028	-0.0289 43.0
24	E09	358.9288	60.7515	1	0.0014	-0.0134 49.9
25	E11	199.5456	16.0973	1	0.0042	-1.9108 37.4
26	E24	172.4665	25.9760	1	0.0027	-0.4737 43.2
27	E31	111.9466	48.0977	1	0.0016	-0.0098 49.8
28	E34	305.1681	18.6196	1	0.0037	0.2002 42.5
29	E36	250.1916	32.1546	1	0.0022	0.0033 45.8
30	C01	137.5061	43.5947	1	0.0018	0.3165 43.0
31	C02	234.7230	38.9551	1	0.0019	0.3956 39.0
32	C03	195.8611	52.6295	1	0.0015	0.2114 42.7
33	C04	121.5219	31.9011	1	0.0023	-0.7755 39.4

Fig. 5 Example of UDIFRES file

2024007.uducres						
0	1.0	2.0	3.0	4.0	5.0	6.0
1	\$GPST	2296	000000	6		
2	G10	311.7356	70.4269	1	0.0012	0.0961 50.9
3	G12	93.5916	41.8635	1	0.0018	-0.1889 46.8
4	G15	95.4434	11.5814	1	0.0056	-0.2458 39.1
5	G18	191.7667	10.8688	1	0.0059	0.2844 45.4
6	G21	316.3169	5.5540	1	0.0106	0.8107 39.2
7	G23	153.2999	66.3348	1	0.0013	-0.1762 50.2
8	G24	47.3302	24.0952	1	0.0028	0.1831 40.8
9	G25	145.1026	43.0441	1	0.0017	-0.0310 46.2
10	G28	239.0651	27.8180	1	0.0025	0.0363 47.0
11	G31	231.9086	3.5013	1	0.0148	-1.0474 37.8
12	G32	311.0185	41.8931	1	0.0017	0.2286 47.9
13	R01	95.7902	32.9276	1	0.0022	0.1762 43.9
14	R02	20.2384	55.6450	1	0.0014	-0.3595 51.2
15	R03	321.8987	22.5926	1	0.0030	-0.6774 44.5
16	R11	29.1169	14.0437	1	0.0047	0.5683 40.9
17	R12	66.0646	67.8161	1	0.0013	-0.0737 51.0
18	R13	183.3851	51.1409	1	0.0015	0.5030 41.3
19	R17	242.6850	7.2759	1	0.0085	-0.3128 41.8
20	R18	288.1601	12.4692	1	0.0052	0.4845 41.2
21	R19	327.9801	4.8559	1	0.0118	-0.9848 32.3
22	E04	73.4307	34.6619	1	0.0021	0.3530 46.9
23	E05	295.9226	25.2773	1	0.0027	0.0280 43.0
24	E09	358.9288	60.7515	1	0.0013	0.0517 49.9
25	E11	199.5456	16.0973	1	0.0041	-0.7620 37.4
26	E24	172.4665	25.9760	1	0.0026	-0.2720 43.2
27	E31	111.9466	48.0977	1	0.0016	-0.0248 49.8
28	E34	305.1681	18.6196	1	0.0036	0.1328 42.9
29	E36	250.1916	32.1546	1	0.0022	-0.0607 45.8
30	C01	137.5061	43.5947	1	0.0017	-0.0465 43.0
31	C02	234.7230	38.9551	1	0.0018	-0.0254 39.0
32	C03	195.8611	52.6295	1	0.0015	-0.0778 42.7
33	C04	121.5219	31.9011	1	0.0022	-0.2531 39.4

Fig. 6 Example of UDUCRES file

## 4 How to Run the MAPS

### 4.1 MATLAB version

Although the MAPS is developed based on MATLAB 2021a, the debugging and use of the MAPS supports almost all MATLAB versions. In addition, it is worth noting that

the MAPS contains the SF modeling capacity, which uses the functions in the wavelet toolbox. Certainly, the users can install the wavelet toolbox or improve the denoise method to obtain more accurate modeling results depending on the users.

## 4.2 Input data

If users want to use their own data to conduct the corresponding multipath analysis and processing using the MAPS, the users need to put their data in the corresponding folder. Meanwhile, if the users want to run the program, the corresponding settings can be changed in the script named “main\_\*.m”. The setting steps are introduced in the following texts below. Fig. 7 shows the corresponding files required by the multipath analysis module. If the users want to establish the C/N0 template function, only the files within the green solid wireframe are needed. In the case of CMC method, only the files within the red solid wireframe are needed. In the case of GFix and IC or GF and IC method, all files in the Fig. 7 are needed except the files within the green solid wireframe.

名称	修改日期	类型
0_obs	2024/12/4 16:51	文件夹
1_sp3	2024/12/4 16:51	文件夹
2_clk	2024/12/4 16:51	文件夹
3_nav	2024/12/4 16:51	文件夹
4_dcb	2024/12/4 16:51	文件夹
5_atx	2024/12/4 16:51	文件夹
6_cn0	2024/12/4 16:51	文件夹
pos_rover	2024/12/4 10:32	MATLAB Data

**Fig. 7** Files needed by the multipath analysis module

Fig. 8 shows the corresponding files required by the MHM modeling and SF modeling in the multipath processing module. The “RES\_MHM.mat” is used for MHM modeling. The “RES\_SF.mat” and “NAV.mat” are used for SF modeling. If the files of “\*.mat” are missing in the folder, the users need to read the residual files and NAV files within the red solid wireframe.

名称	修改日期	类型	大小
0_ddres	2024/12/4 16:57	文件夹	
1_udifres	2024/12/4 16:57	文件夹	
2_uducres	2024/12/4 16:57	文件夹	
3_nav	2024/12/4 16:57	文件夹	
NAV	2024/12/4 10:30	MATLAB Data	462 KB
RES_MHM	2024/12/4 10:21	MATLAB Data	975,913 KB
RES_SF	2024/12/4 10:29	MATLAB Data	269,812 KB

**Fig. 8** Files needed by the MHM modeling and SF modeling in the multipath processing module

## 4.3 Multipath analysis

The CMC method, GFix and IC method, GF and IC method, or the modeling of C/N0 template function needs to be set and executed in script named “main\_MPAnalysis.m”.

The following demonstrates the corresponding steps to run the “main\_MPAnalysis.m” with sample data.

### Step 1: Constants.

```
%% -----【Constants】-----
CONST.clight=299792458; %speed of light (m/s)
CONST.GPS_F1 = 1.57542E9; %L1 frequency (Hz)
CONST.GPS_F2 = 1.22760E9; %L2 frequency (Hz)
CONST.GPS_F5 = 1.17645E9; %L5 frequency (Hz)
CONST.GAL_F1 = 1.57542E9; %E1 frequency (Hz)
CONST.GAL_F5a = 1.17645E9; %E5a frequency (Hz)
CONST.GAL_F5b = 1.20714E9; %E5b frequency (Hz)
CONST.BDS_F1I = 1.561098E9; %B1I frequency (Hz)
CONST.BDS_F2I = 1.20714E9; %B2I frequency (Hz)
CONST.BDS_F3I = 1.26852E9; %B3I frequency (Hz)
CONST.BDS_F1C = 1.57542E9; %B1C frequency (Hz)
CONST.BDS_F2a = 1.17645E9; %B2a frequency (Hz)

CONST.GPS_L1=CONST.clight/CONST.GPS_F1; %wavelength (m)
CONST.GPS_L2=CONST.clight/CONST.GPS_F2;
CONST.GPS_L5=CONST.clight/CONST.GPS_F5;
CONST.GAL_L1=CONST.clight/CONST.GAL_F1;
CONST.GAL_L5a=CONST.clight/CONST.GAL_F5a;
CONST.GAL_L5b=CONST.clight/CONST.GAL_F5b;
CONST.BDS_L1C=CONST.clight/CONST.BDS_F1C;
CONST.BDS_L2a=CONST.clight/CONST.BDS_F2a;
CONST.BDS_L1I=CONST.clight/CONST.BDS_F1I;
CONST.BDS_L2I=CONST.clight/CONST.BDS_F2I;
CONST.BDS_L3I=CONST.clight/CONST.BDS_F3I;
....
```

### Step 2: Settings.

```
%% -----【Settings】-----
%---model
%Please select whether to perform CMC/GFixIC/GFIC analysis and estimation.
%1:CMC 2:GFixIC 3:GFIC 4: CNO
settings.model=3;
%---plot
%Please choose whether to plot figure. 0:NO 1:YES
settings.fig=0;

***** 【Settings of CMC】 *****
%If settings.model=1, the following settings are required;
%if not, the following settings can be ignored.
%---navsys
%Please select satellite systems you want to support. 0:NO 1:YES
settings.sys.gps=1;
settings.sys.gal=1;
settings.sys.bds=1;
%---frequency
%Please set which two frequencies are used to calculate the CMC of GPS.
%(GPS_F1/GPS_F2/GPS_F5)
gpsf1=CONST.GPS_F1; gpsf2=CONST.GPS_F2;
%Please set which two frequencies are used to calculate the CMC of GAL.
%(GAL_F1/GAL_F5a/GAL_F5b)
galf1=CONST.GAL_F1; galf2=CONST.GAL_F5a;
%Please set which two frequencies are used to calculate the CMC of BDS.
%(BDS_F1I/BDS_F2I/BDS_F3I/BDS_F1C/BDS_F2a)
bdsf1=CONST.BDS_F1I; bdsf2=CONST.BDS_F3I;
```

### Step 3: Set the file path. Please prepare the corresponding data files and place them in the corresponding folder.

```

%% -----【Addpath】-----
%---File path
%obs files
o_ipath='0_Input\0_MPanalysis\0_obs';
%sp3 files
s_ipath='0_Input\0_MPanalysis\1_sp3';
%clk files
c_ipath='0_Input\0_MPanalysis\2_clk';
%nav files
n_ipath='0_Input\0_MPanalysis\3_nav';
%dcb files
d_ipath='0_Input\0_MPanalysis\4_dcb';
%atx files
a_ipath='0_Input\0_MPanalysis\5_atx';
%C/N0 file
cn0_ipath='0_Input\0_MPanalysis\6_cn0';
%position of rover
p_ipath='0_Input\0_MPanalysis\pos_rover.mat';
%---Addpath
addpath('1_Read');
addpath('2_Preprocess');
addpath('3_MPanalysis');
addpath('6_Plot');
addpath('8_Tool');

```

**Step 4: Run the CMC method, GFix and IC method, GF and IC method, or the modeling of C/N0 template function.**

**Step 5: Plot the corresponding results of the CMC method, GFix and IC method, GF and IC method, or the modeling of C/N0 template function.**

#### 4.4 MHM modeling

The MHM modeling needs to be set and executed in the script named “main\_MHMMModel.m”. The using of DDRES, supporting of four systems and modeling of five types of MHM models are as examples to demonstrate the corresponding steps in the following texts. It is noted that the MHM modeling involves the selection of different systems, different frequencies, and different residual types, which are all located in the setting part of the script. Hence, the setting part is mainly introduced here, and the modeling part is briefly introduced.

**Step 1: Settings.**

(1) Set the supported satellite systems.

```

%% -----【Settings】-----
%MHMmodel
%Satellite revisiting period; GREC
%1. GPS: 1day; 2. GLO: 8day; 3. GAL: 10day; 4. BDS: 1day (GEO/IGSO) 7day (MEO)
%---navsys
%Please select satellite systems you want to support.          0:NO 1:YES
settings.sys.gps=1;
settings.sys.glo=1;
settings.sys.gal=1;
settings.sys.bds=1;

```

(2) Set the supported frequencies. It is noted that the settings of supported frequencies should obey the settings of supported systems.

```

%---frequency
%Please select the frequencies you want to support.          0:NO 1:YES
%GPS
settings.freq.L1=1;
settings.freq.L2=1; %When it is DD residual, L2 actually represents L5.
%GLO
settings.freq.G1=1;
settings.freq.G2=1;
%GAL
settings.freq.E1=1;
settings.freq.E5a=1;
%BDS
settings.freq.B1I=1;
settings.freq.B3I=1;
settings.freq.B1C=1;
settings.freq.B2a=1;

```

- (3) Set the supported MHM models. It is noted that multiple models can be set here at the same time.

```

%Please select the MHM model you want to establish.
%MHM refers to traditional MHM.          0:NO 1:YES
%SMHM refers to GEO, IGS0 and MEO satellite MHM of BDS. 0:NO 1:YES
%FMHM refers to GPS/Galileo/BDS3 overlapping frequency MHM. 0:NO 1:YES
%PMHM refers to precision MHM.          0:NO 1:YES
%TMHM refers to the trend surface analysis of MHM.      0:NO 1:YES
settings.model.Trad=1;
settings.model.Prec=1;
settings.model.Sat=1;
settings.model.Freq=1;
settings.model.Tre=1;

```

- (4) Set the type of residual used for modeling and choose whether to use residuals from fixed solution or float solution.

```

%---Tres
%Please select the residual type to use.
%0: no res 1:ddres 2:udifres 3:uducres
%When Tres is 0, it means that the sample data (RES_MHM.mat)
%that has been read is used
settings.resType=1;
%---Q
%Please choose to use the residual of fixed solution or float solution.
%1:fixed 2:float
settings.Q=1;

```

- (5) Set the grid resolution of the model to be established.

```

%---Grid resolution of MHM.
%Please select the grid resolution of MHM.    1:0.5° ×0.5°   2:1° ×1°
settings.gridReso=2;
%
```

- (6) Set the type of plotting.

```

%---Plot
%Please select the type of plotting you want. 0: No plot 1:2D sky plot
%                                              2:2D plane 3:3D sky plot
settings.figure=1;
%Please choose whether to plot a figure of code residuals. 0:NO 1:YES
settings.fig.code=1;
%Please choose whether to plot a figure of phase residuals. 0:NO 1:YES
settings.fig.phase=1;

```

**Step 2: Set the file path. Please prepare the corresponding data files and place them in the corresponding folder.**

```
%---File path
%ddres files
dd_ipath='0_Input\1_MHMSFmodel\0_ddres';
%udifres files
udif_ipath='0_Input\1_MHMSFmodel\1_udifres';
%uducres files
uduc_ipath='0_Input\1_MHMSFmodel\2_uducres';
%---Addpath
addpath('1_Read\');
addpath('2_Preprocess\');
addpath('4_MHMmodel\');
addpath('6_Plot\');
addpath('8_Tool\');
...
```

**Step 3: Run the MHM modeling. This step is divided into three sub-steps: reading residuals, modeling, and plotting.**

- (1) Reading residuals. According to the above settings, the DDRES will be read. Here, the ‘SD\_fix’ stores the SD residuals of fixed solutions, which is assigned to ‘RES’. (Note: This step may take a long time.)
- (2) Modeling. The used examples establish five types of models, and the modeling results are stored in the corresponding structures.
- (3) Plotting. The corresponding plotting examples will be given in the Chapter 5.

## 4.5 SF modeling

The SF modeling needs to be set and executed in the script named “main\_SFModel.m”. The using of UDUCRES, supporting of GPS, Galileo, and BDS systems, and modeling of two types of SF models are as examples to demonstrate the corresponding steps in the following texts. It is noted that the SF modeling involves the selection of different systems, different frequencies, and different residual types, which are all located in the setting part of the script. Hence, the setting part is mainly introduced here, and the modeling part is briefly introduced.

### Step 1: Settings.

- (1) Select the supported satellite systems. It is noted that only GPS, Galileo, and BDS systems are supported.

```
%% -----【Settings】-----
%SFmodel
%Satellite revisiting period; GEC
%1. GPS: 1day; 2. GAL: 10day; 3. BDS: 1day (GEO/IGSO) 7day (MEO)
%---navsys
%Please select satellite systems you want to support.          0:NO  1:YES
settings.sys.gps=1;
settings.sys.gal=1;
settings.sys.bds=1;
```

- (2) Set the supported frequencies. It is noted that the settings of supported frequencies should obey the settings of supported systems.

```

%---frequency
%Please select the frequencies you want to support.          0:NO  1:YES
%GPS
settings.freq.L1=1;
settings.freq.L2=1; %When it is DD residual, L2 actually represents L5.
%GAL
settings.freq.E1=1;
settings.freq.E5a=1;
%BDS
settings.freq.B1l=1;
settings.freq.B3l=1;
settings.freq.B1C=1;
settings.freq.B2a=1;

```

- (3) Set the supported SF models. It is noted that multiple models can be set here at the same time.

```

%Please select the SF model you want to establish.
%SF refers to the traditional SF model.          0:NO  1:YES
%SF_Win refers to the window matching SF model. 0:NO  1:YES
settings.model.SF=1;
settings.model.SFWin=0;

```

- (4) Set the type of residual used for modeling and choose whether to use residuals from fixed solution or float solution.

```

%---resType
%Please select the residual type to use.
%0: no res  1:ddres  2:udifres  3:uducres
%When resType is 0, it means that the sample data (res_SF.mat)
%that has been read is used
settings.resType=1;
%---Q
%Please choose to use the residual of fixed solution or float solution.
%1:fixed  2:float
settings.Q=1;

```

- (5) Set the window size (if the SF\_Win model is not supported, the window size can be set to 0.)

```

%---Window size
%Please set the size of the window.
%eg:window = 60 * 10, which means every 10 minutes.
settings.Win=60*10;

```

**Step 2: Set the file path. Please prepare the corresponding data files and place them in the corresponding folder.**

```

%---File path
%ddres files
dd_ipath='0_Input\1_MHMSFmodel\0_ddres';
%udifres files
udif_ipath='0_Input\1_MHMSFmodel\1_udifres';
%uducres files
uduc_ipath='0_Input\1_MHMSFmodel\2_uducres';
%brdm files
n_ipath='0_Input\1_MHMSFmodel\3_nav';
%---Addpath
addpath('1_Read\');
addpath('2_Preprocess\');
addpath('5_SFmodel\');
addpath('6_Plot\');
addpath('8_Tool\');

```

**Step 3: Run the SF modeling.** This step is divided into four sub-steps: reading residuals, reading broadcast ephemeris, modeling, and plotting.

- (1) Reading residuals. According to the above settings, the UDUCRES will be read. Here, the ‘UDUC’ and ‘UDUC1’ store the undifferenced and uncombined residuals, which are assigned to ‘RES’ and ‘RES1’, respectively. (Note: This step may take a long time.)
- (2) Reading broadcast ephemeris. The broadcast ephemeris is used to calculate the satellite period.
- (3) Modeling. The used examples establish two types of models, and the modeling results are stored in the corresponding structures.
- (4) Plotting. The time series plot of the residuals of each satellite is plotted.

## 5 Plotting function

All the plotting functions are stored in **6\_Plot** folder, and the plotting functions are involved in the multipath analysis and processing modules of the MAPS. It is noted that the corresponding plotting settings can be set in the corresponding script. Here, the plotting types supported in the MAPS and the corresponding examples are shown in the following texts.

### 5.1 Plotting of multipath analysis

#### 5.1.1 CMC method

##### (1) Time series plot

CMC time series of each GPS satellite

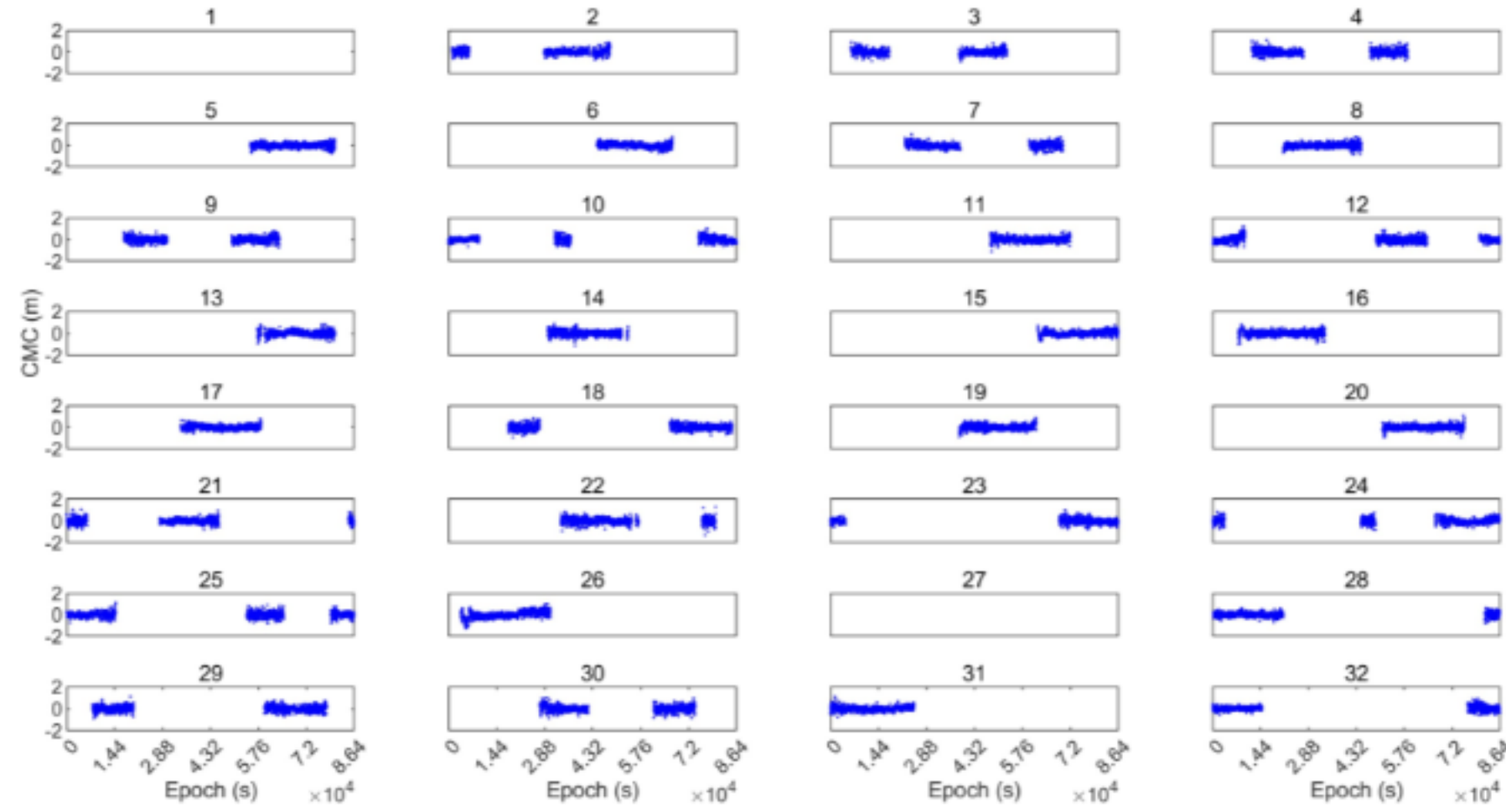


**Fig. 9** CMC time series of GPS satellites

CMC time series of each GAL satellite

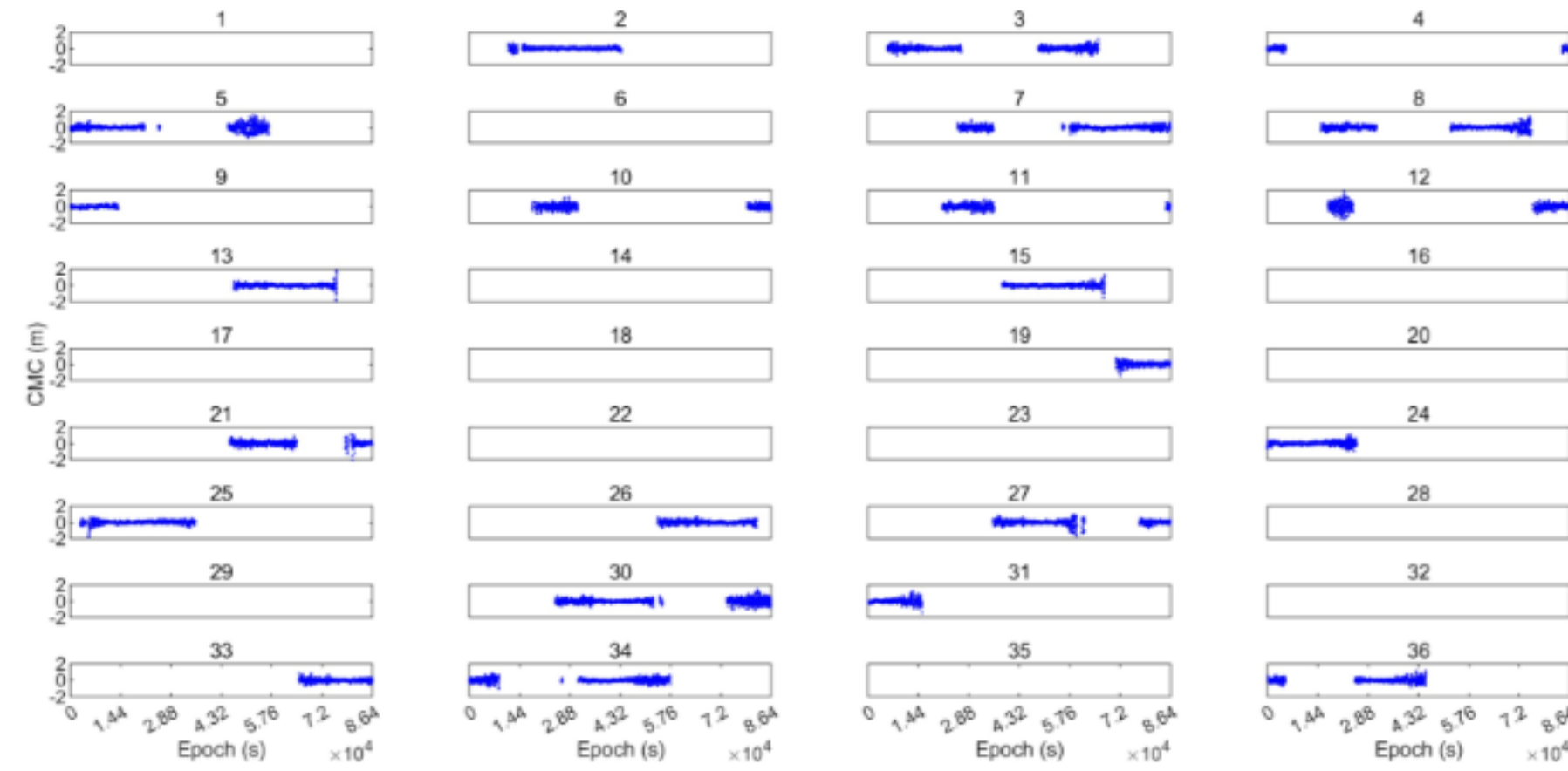


**Fig. 10** CMC time series of Galileo satellites

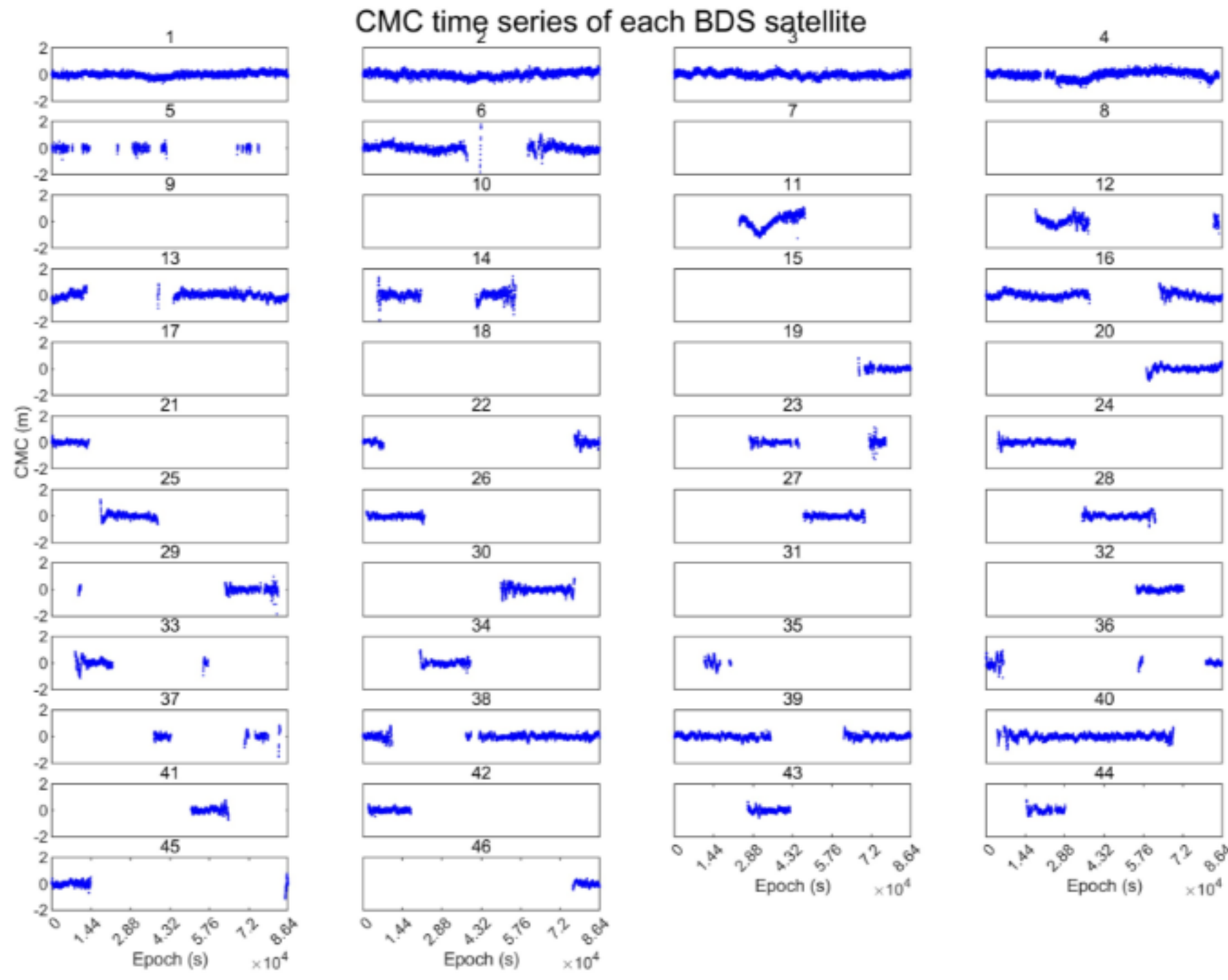


**Fig. 11** CMC time series of BDS satellites

## (2) Sky plot

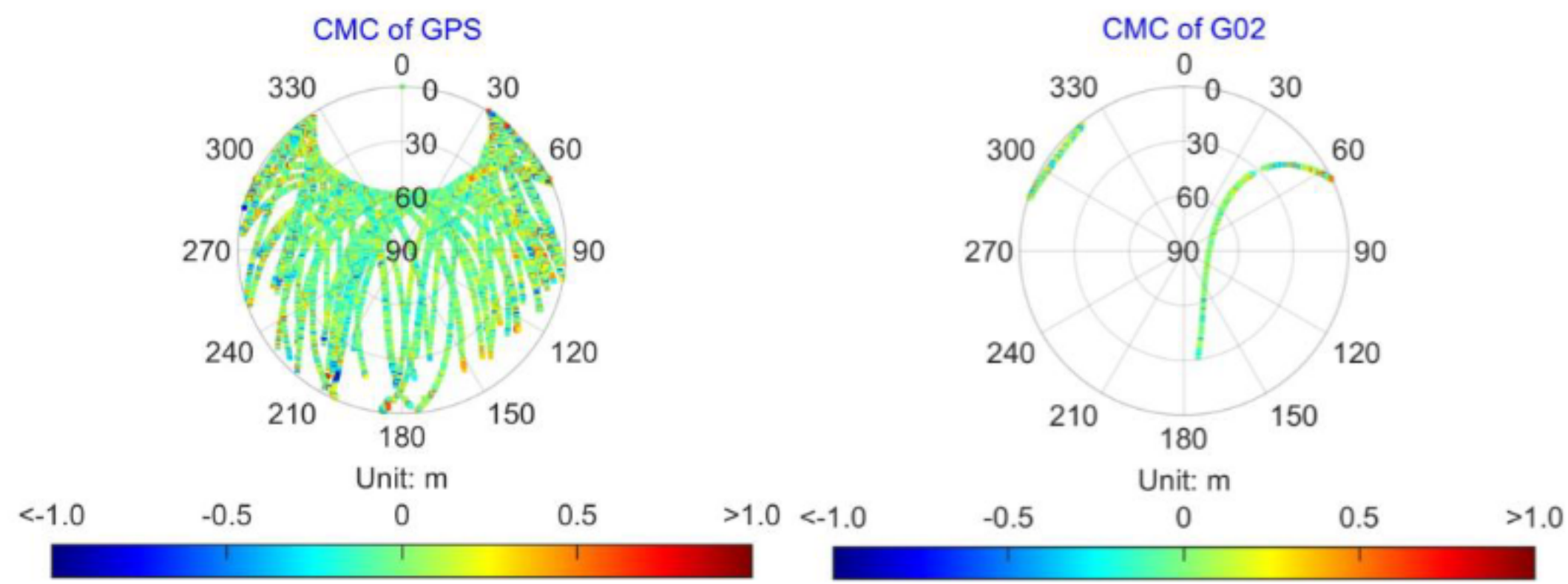


**Fig. 12** CMC sky plot of GPS satellites

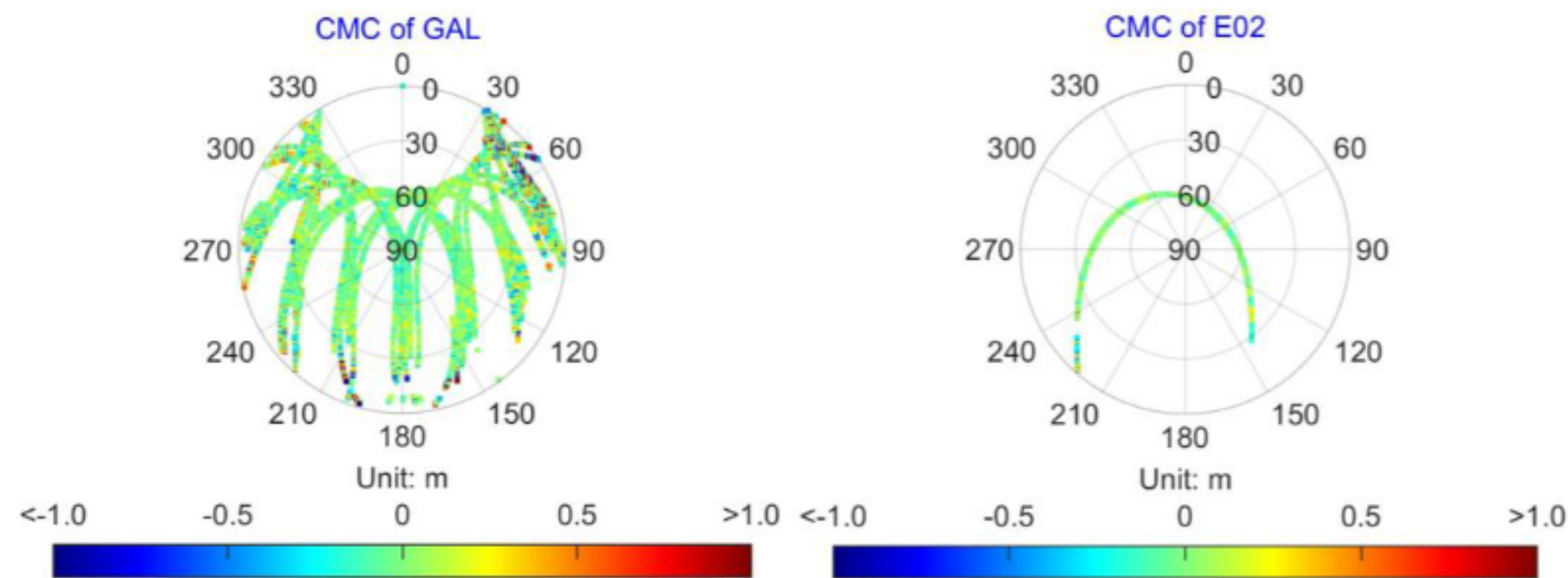


**Fig. 13** CMC sky plot of Galileo satellites

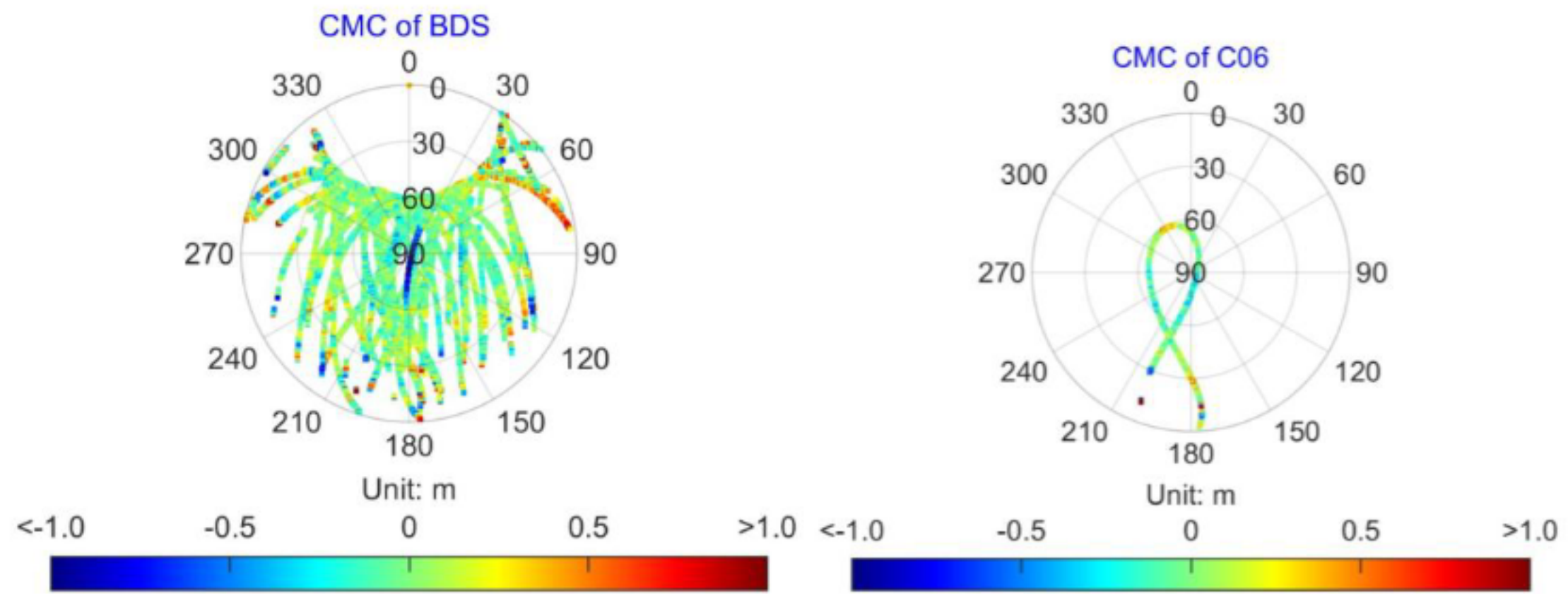


**Fig. 14** CMC sky plot of BDS satellites

### 5.1.2 GFix and IC method

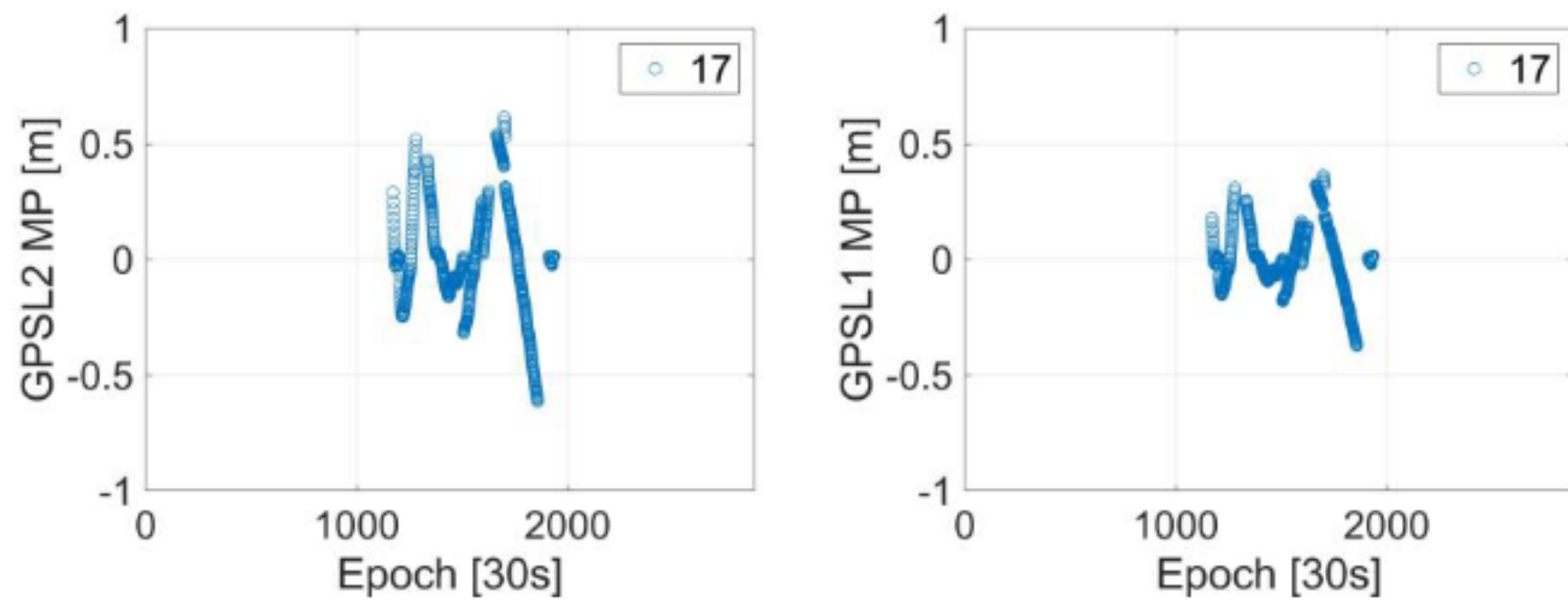


**Fig. 15** Multipath time series of L1 and L2 of G17 satellite

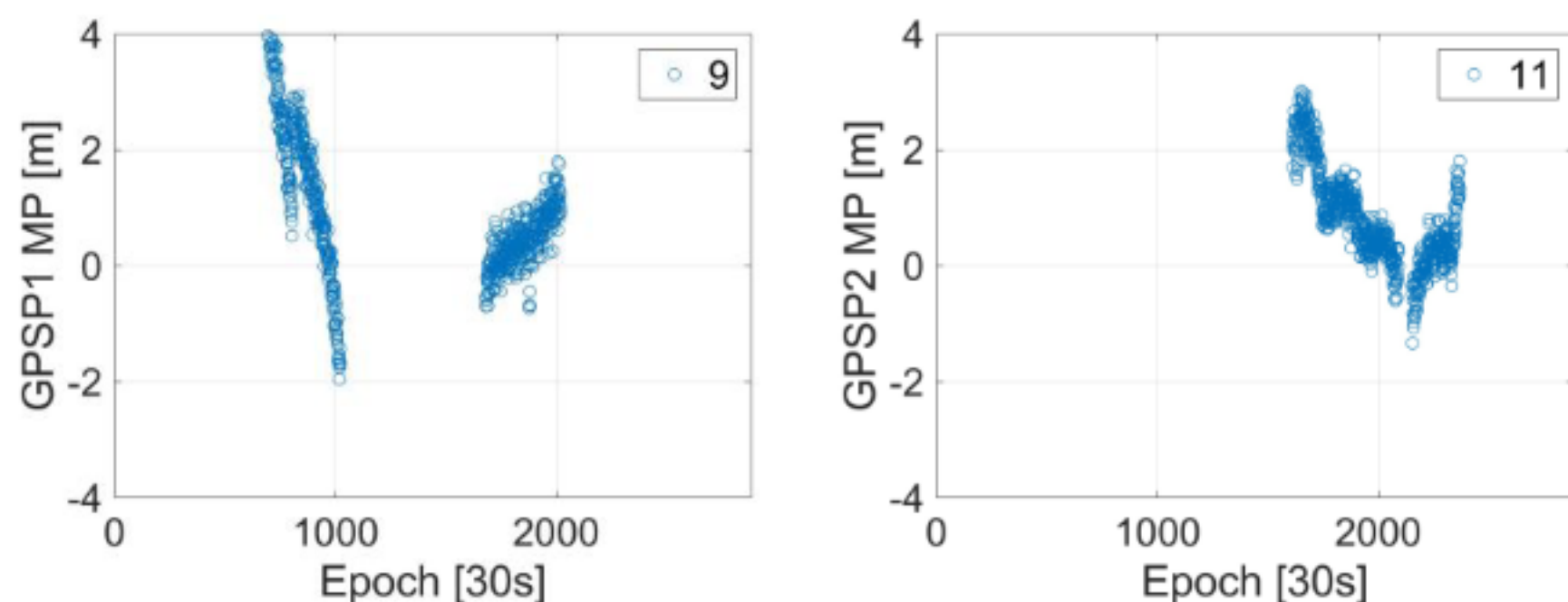


**Fig. 16** Multipath time series of P1 of G09 satellite and P2 of G11 satellite

### 5.1.3 GF and IC method

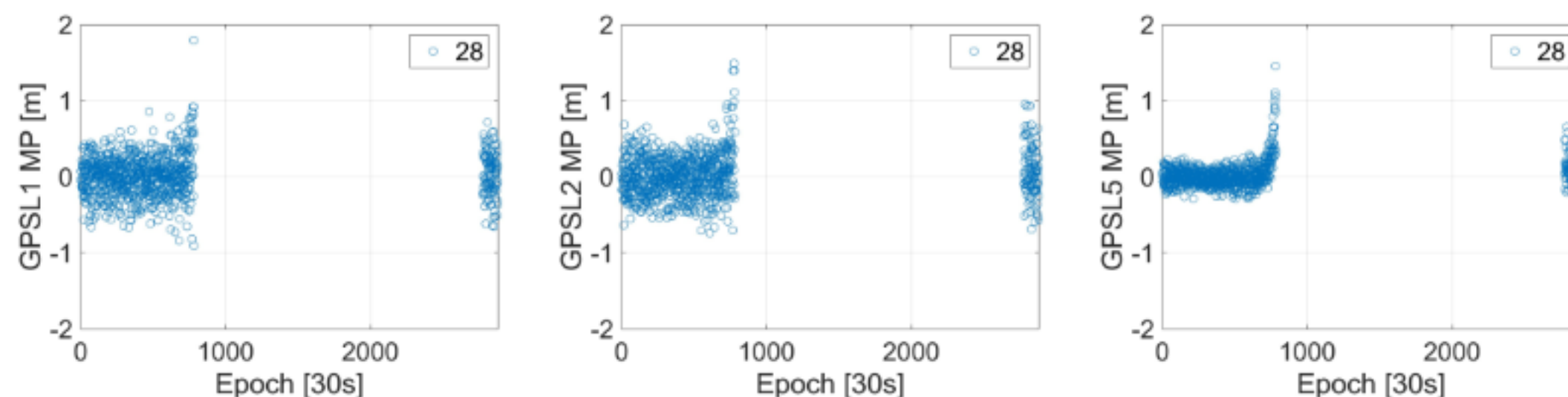


**Fig. 17** Multipath time series of G28 satellite

#### 5.1.4 C/N0 template function

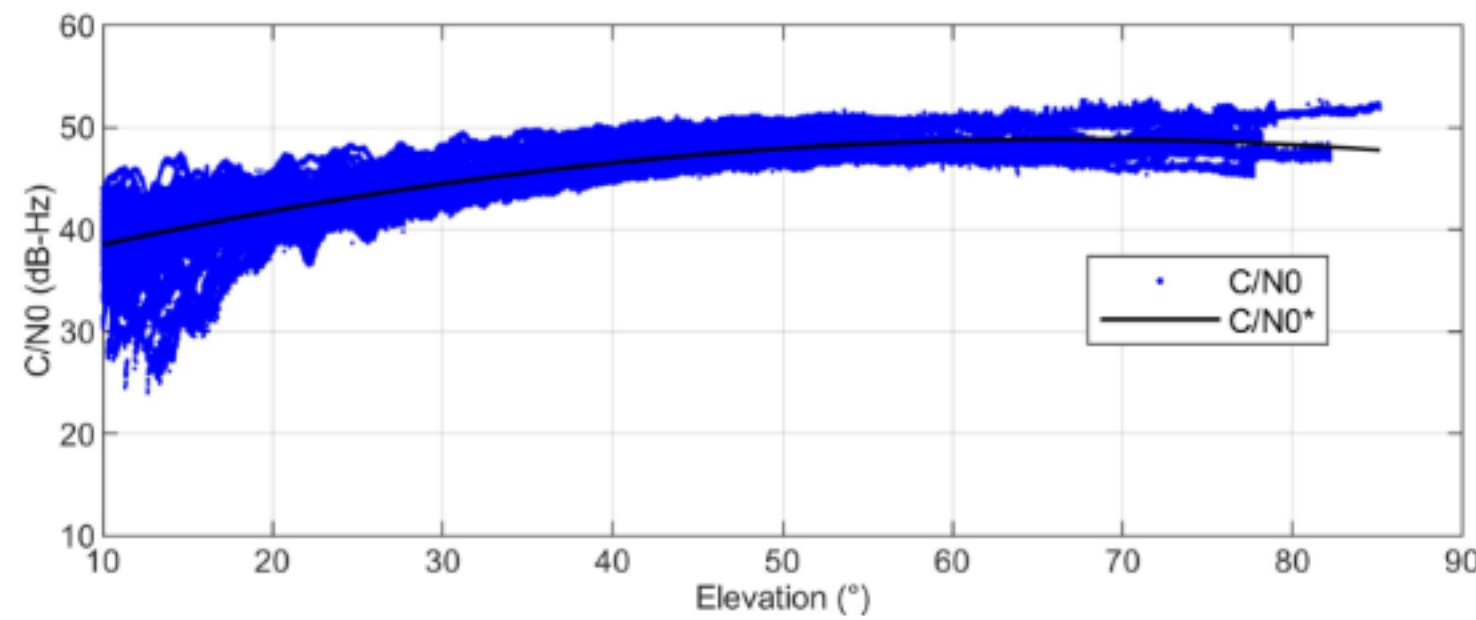


**Fig. 18** C/N0 values and C/N0 template function

### 5.2 Plotting of MHM modeling

For the MHM modeling part, the plotting of MHM, PMHM, SMHM, and FMHM are supported. The plotting types include 2D sky plot, 2D plane, and 3D sky plot.

#### 5.2.1 2D sky plot

##### 1. MHM

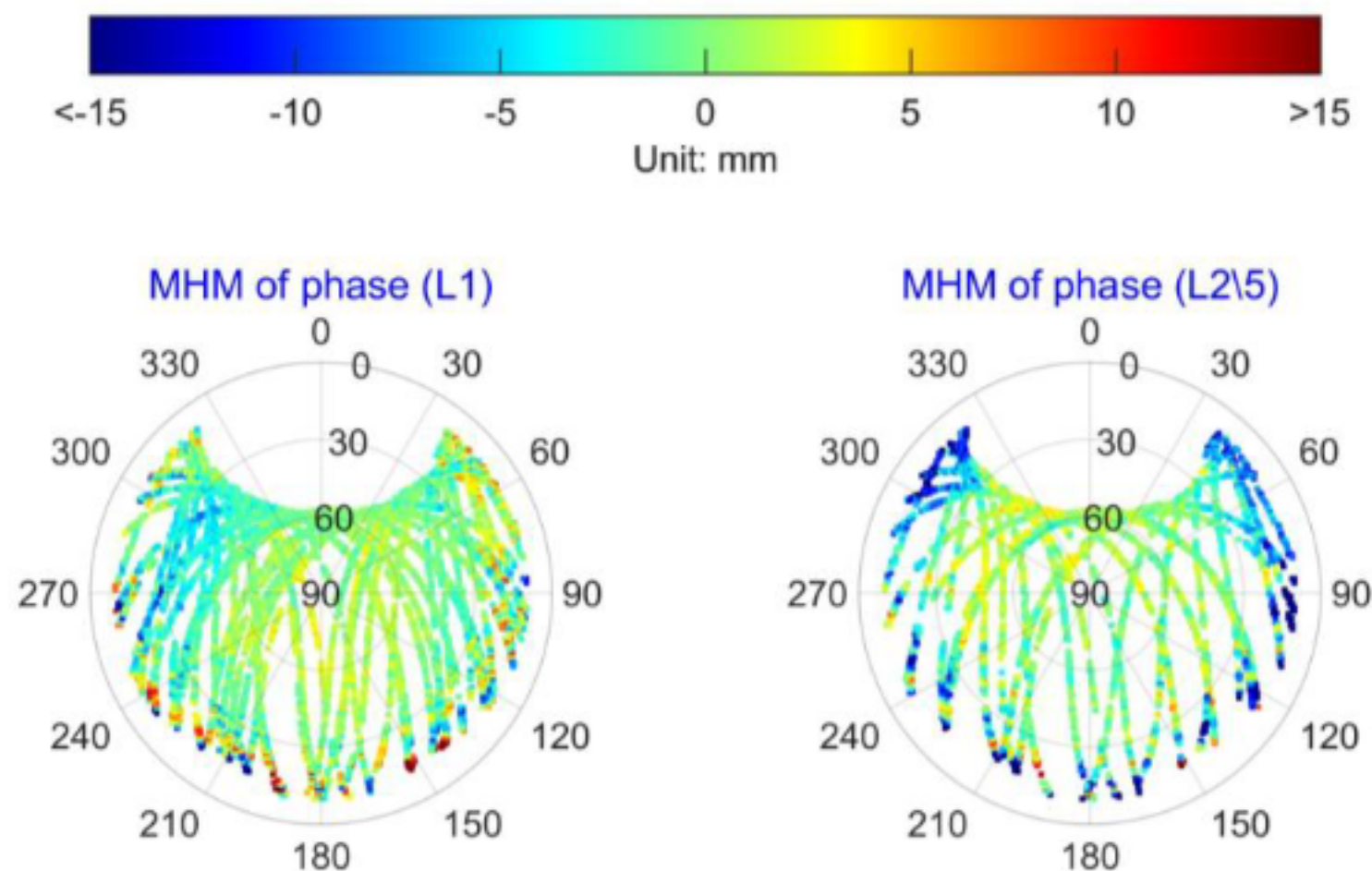


**Fig. 19** 2D sky plot of phase MHM for GPS

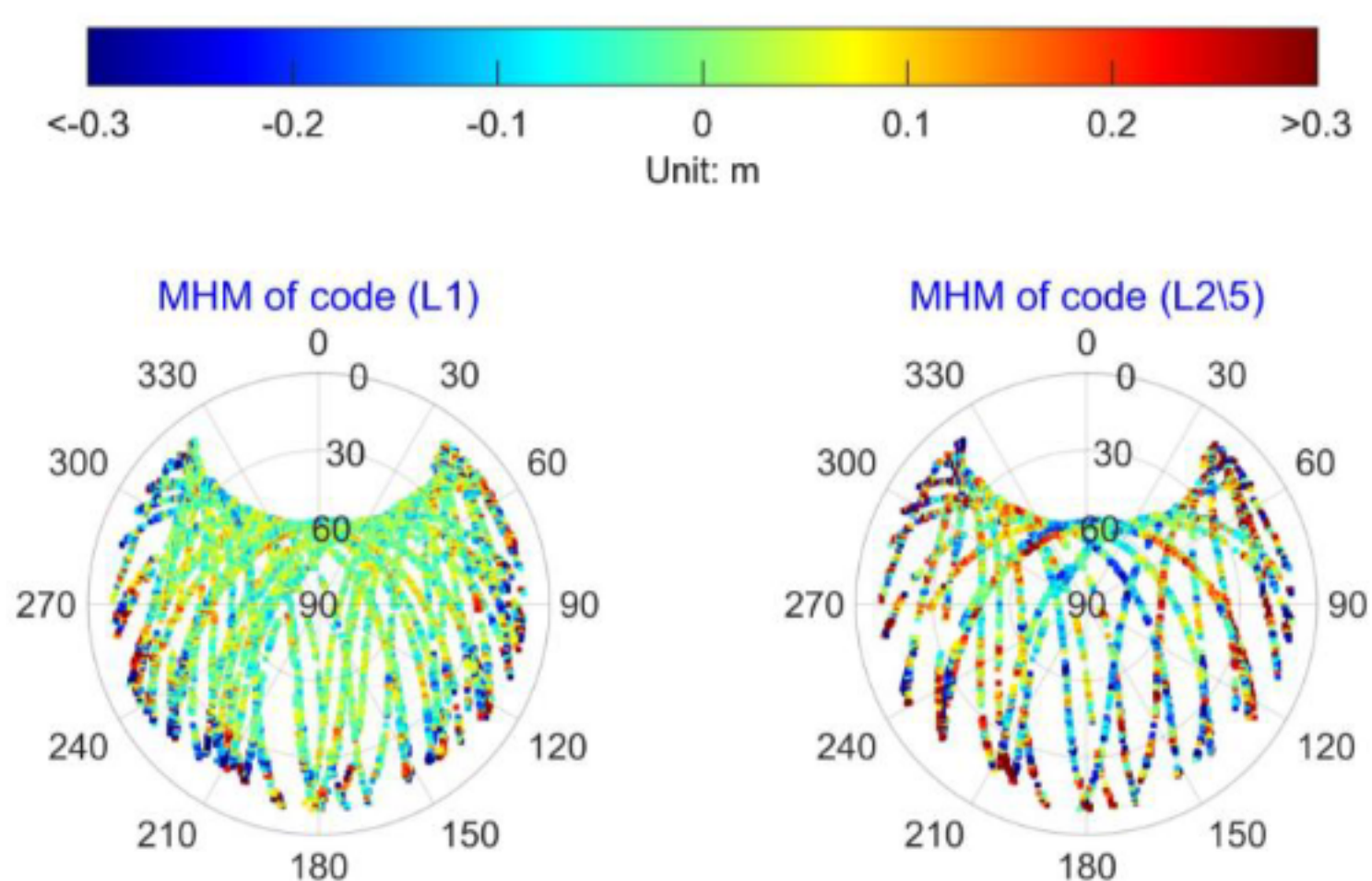


**Fig. 20** 2D sky plot of code MHM for GPS

## 2. PMHM

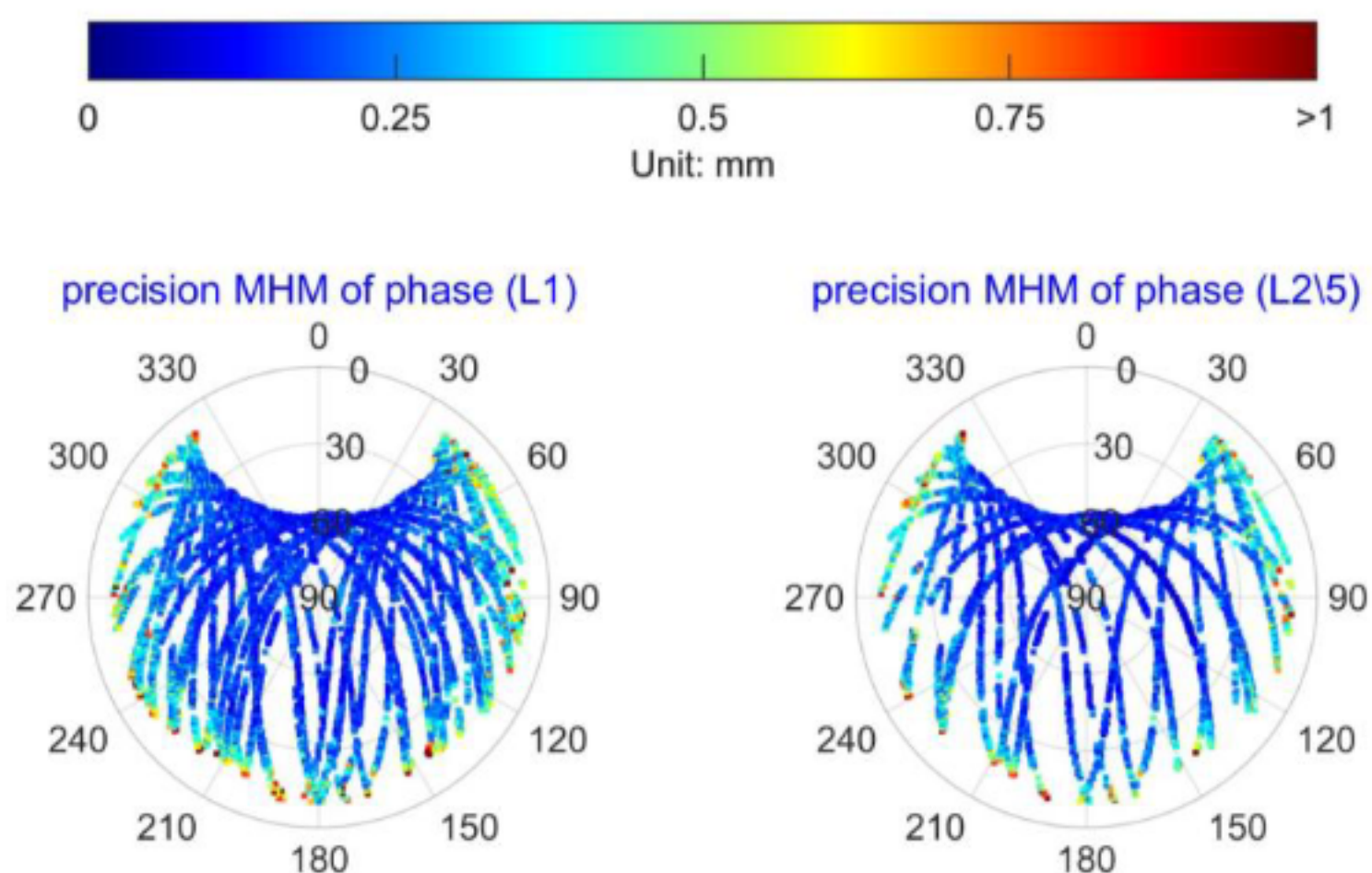


**Fig. 21** 2D sky plot of phase PMHM for GPS

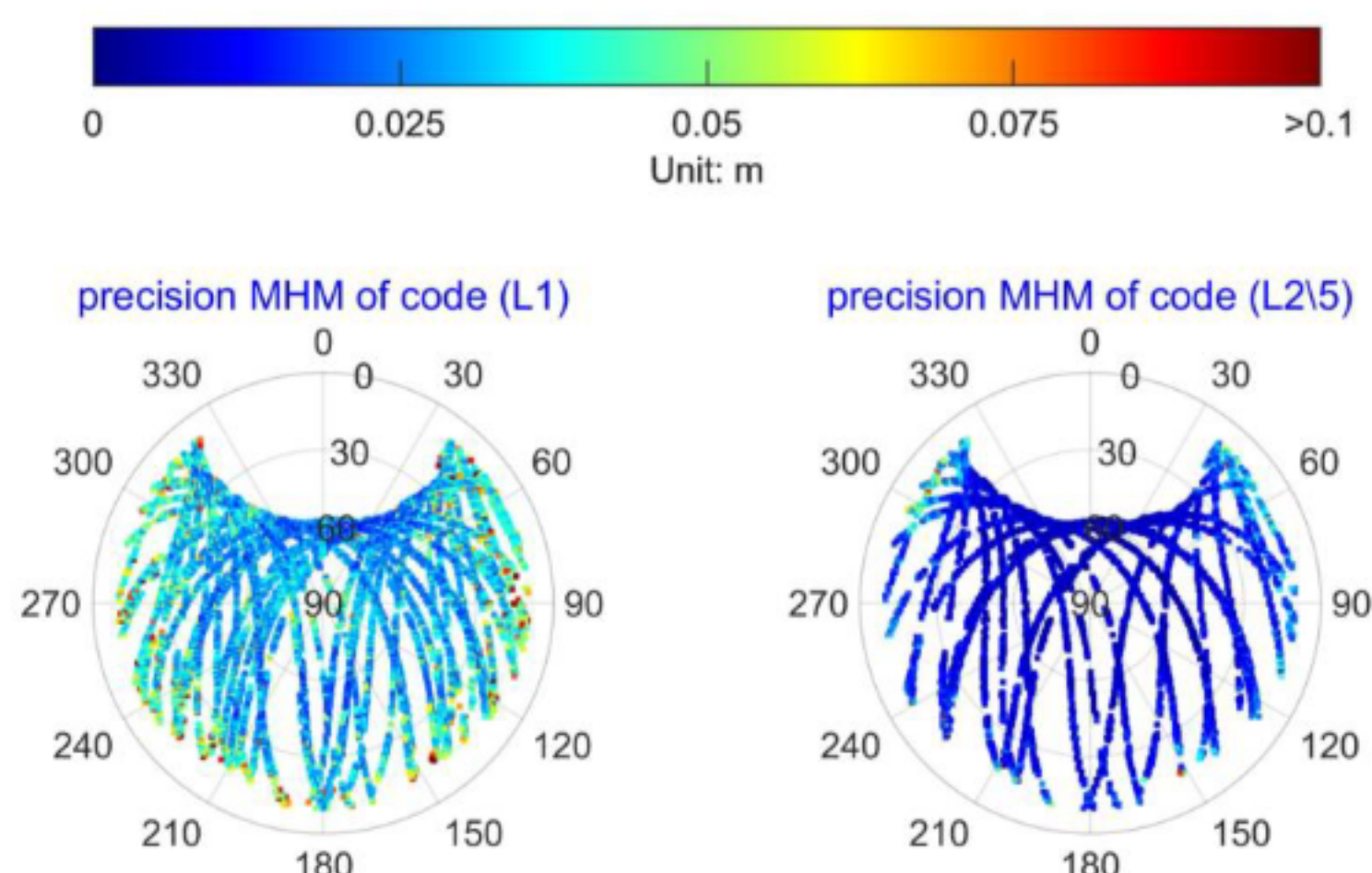


**Fig. 22** 2D sky plot of code PMHM for GPS

## 3. SMHM

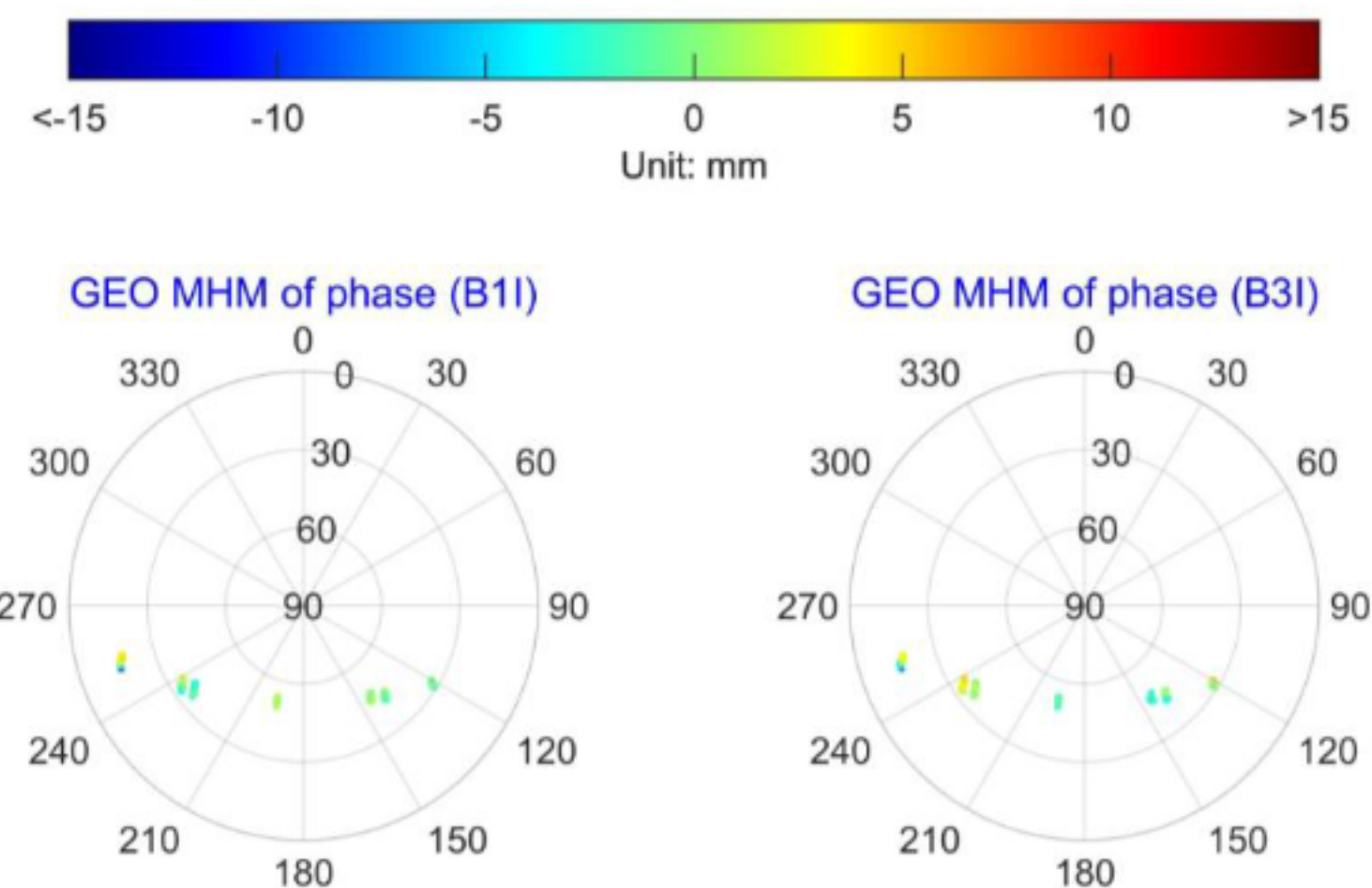


**Fig. 23** 2D sky plot of phase MHM for BDS GEO satellites

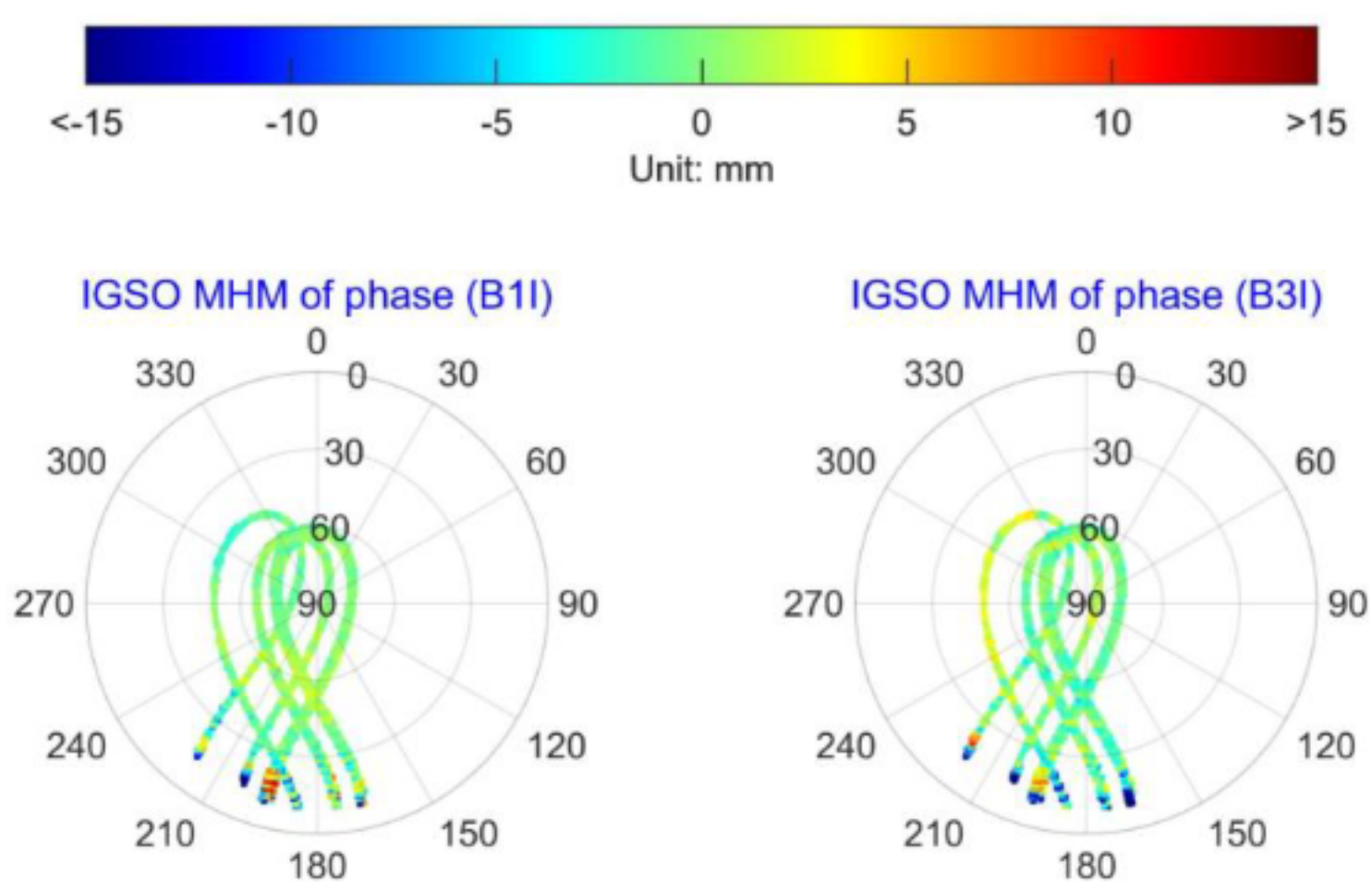


**Fig. 24** 2D sky plot of phase MHM for BDS IGSO satellites

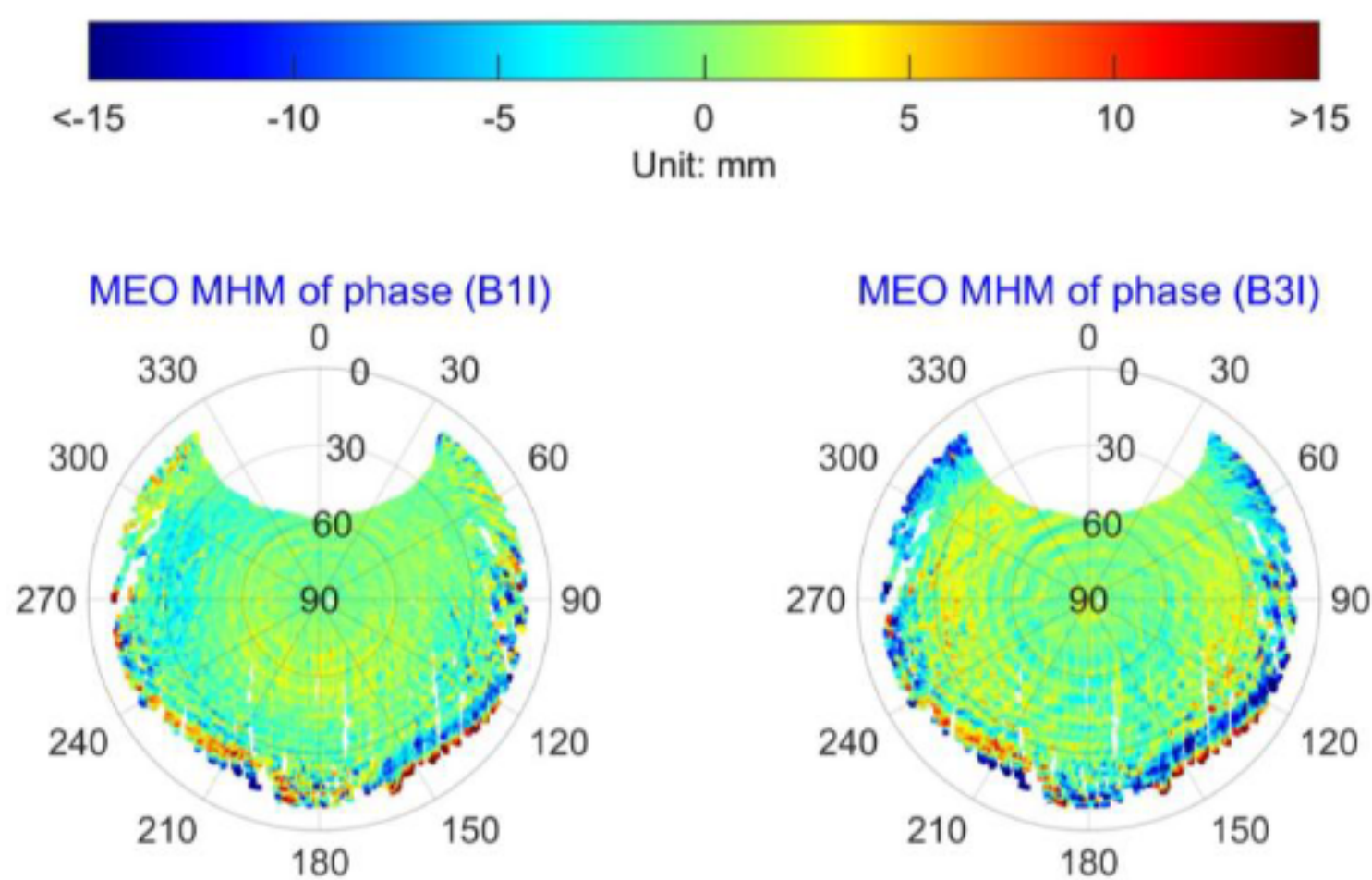


**Fig. 25** 2D sky plot of phase MHM for BDS MEO satellites

#### 4. FMHM

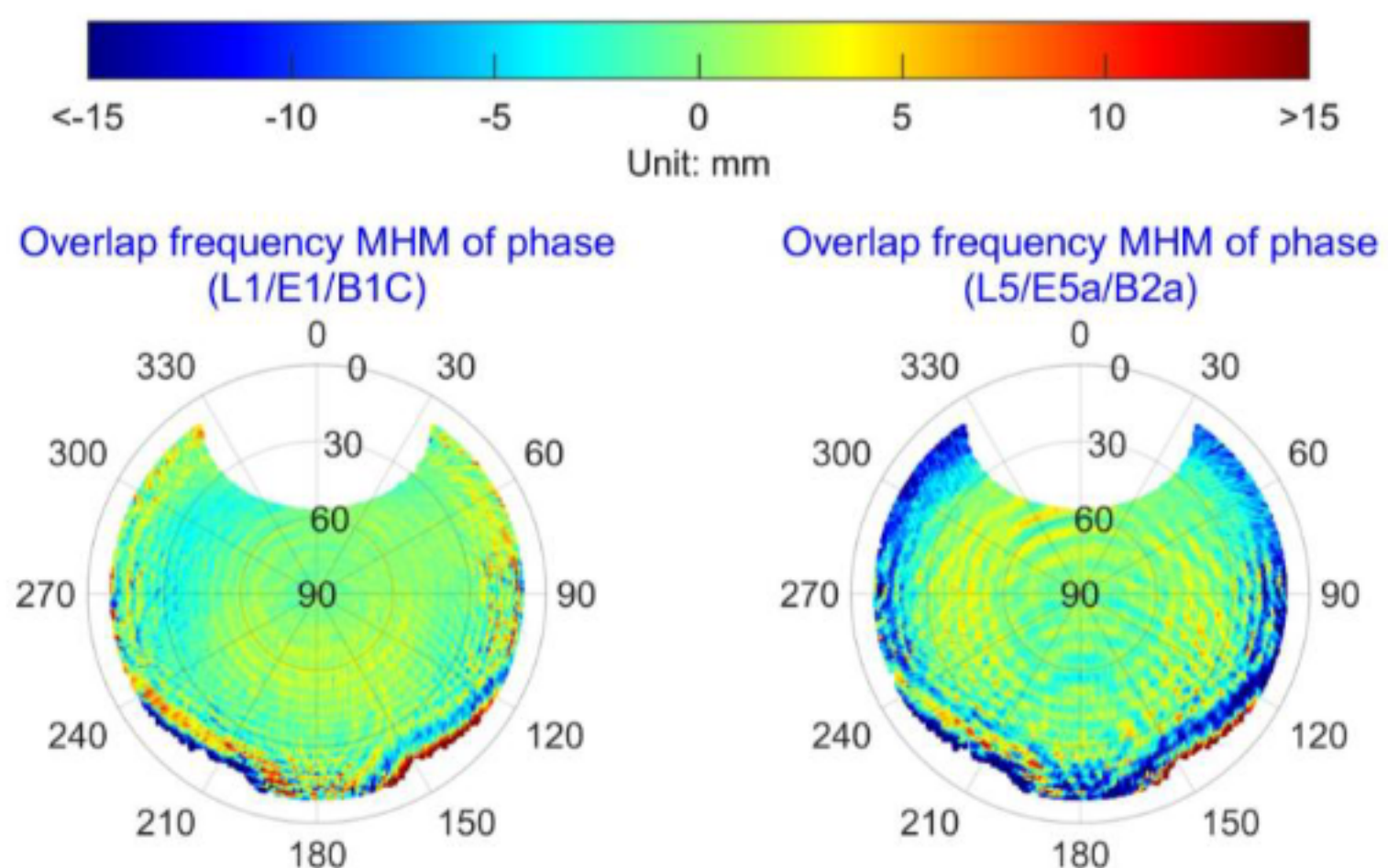


**Fig. 26** 2D sky plot of phase FMHM

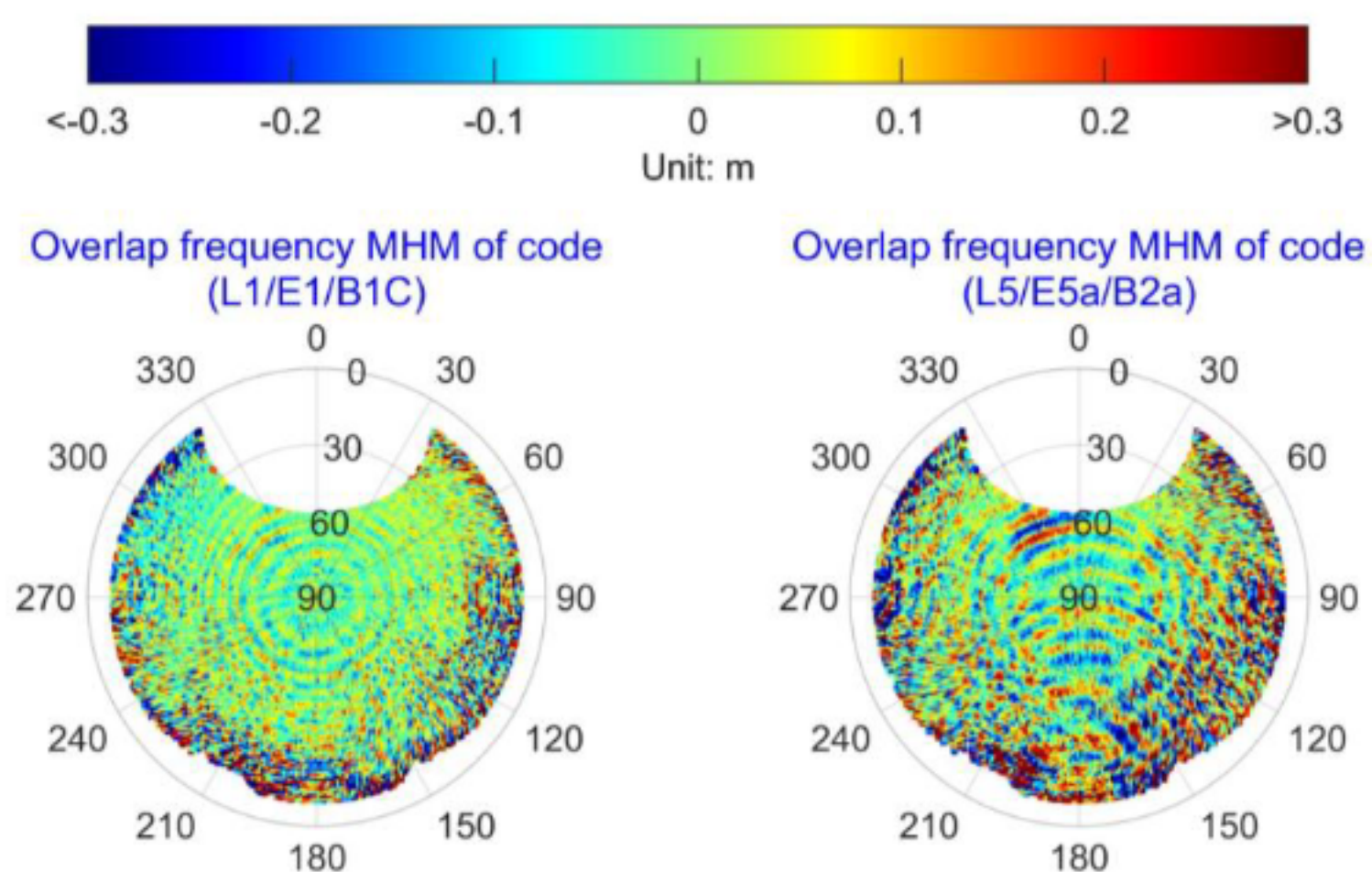


**Fig. 27** 2D sky plot of code FMHM

### 5.2.2 2D plane plot

#### 1. MHM

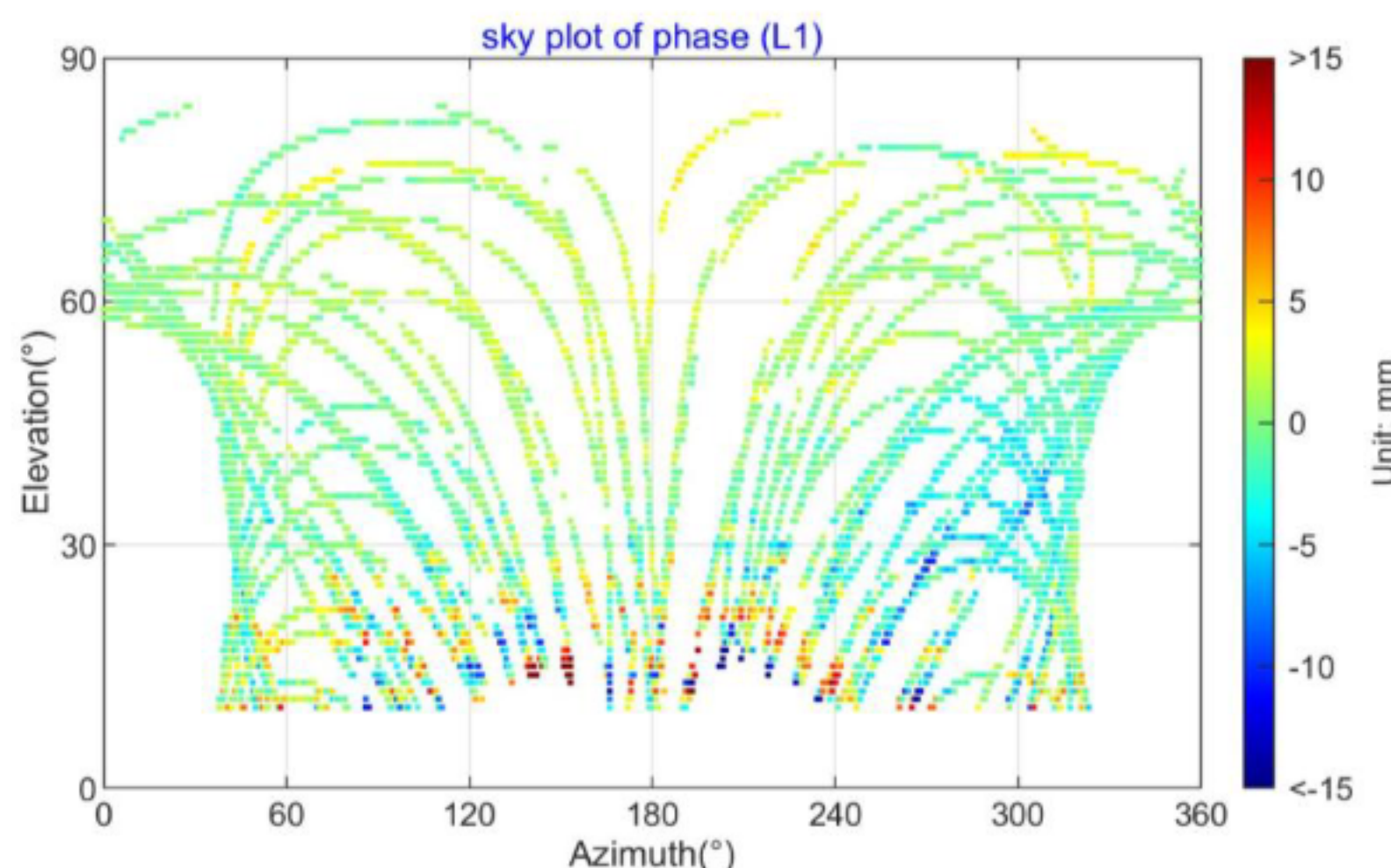


**Fig. 28** 2D plane plot of phase MHM for GPS

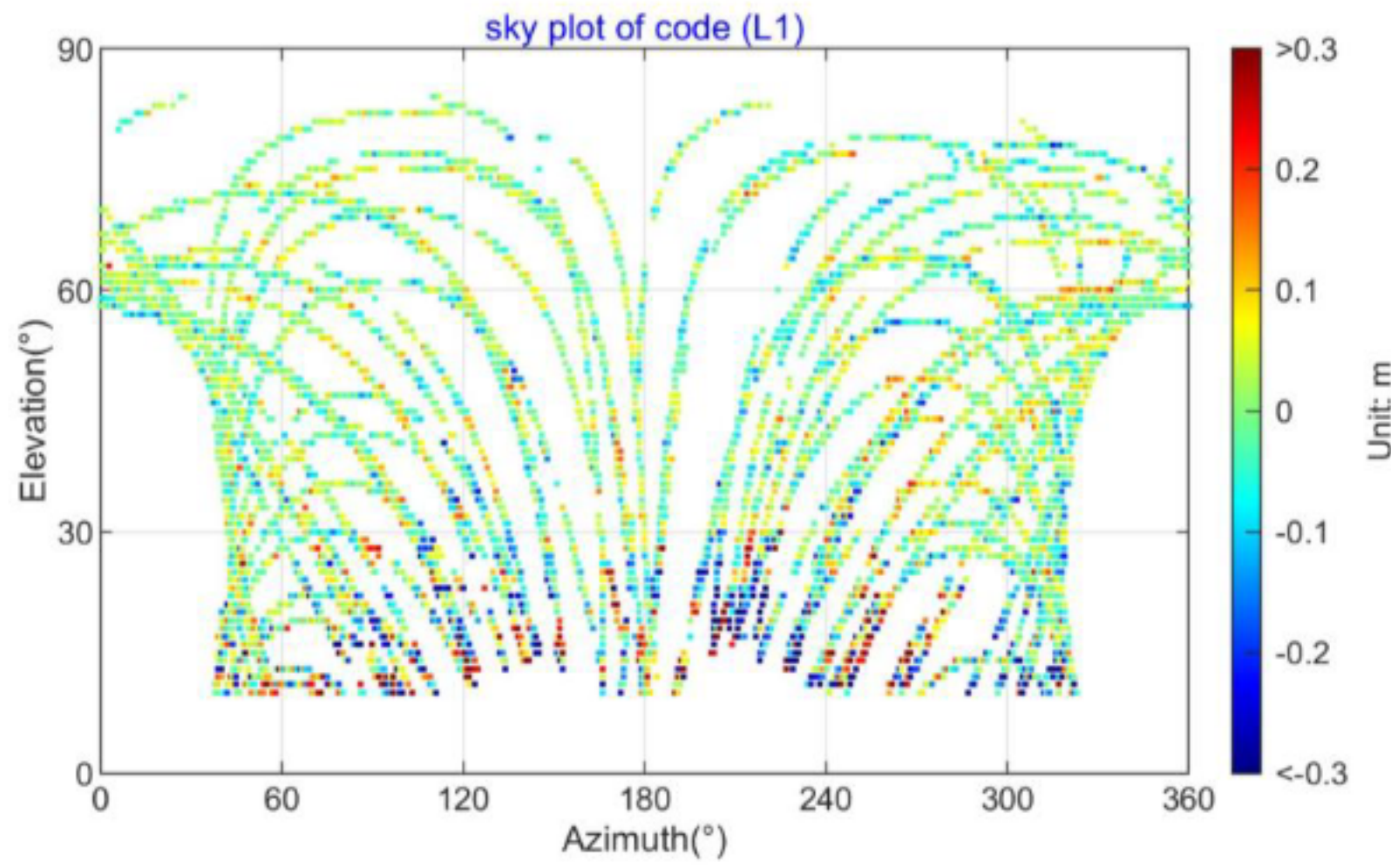


**Fig. 29** 2D plane plot of code MHM for GPS

## 2. PMHM

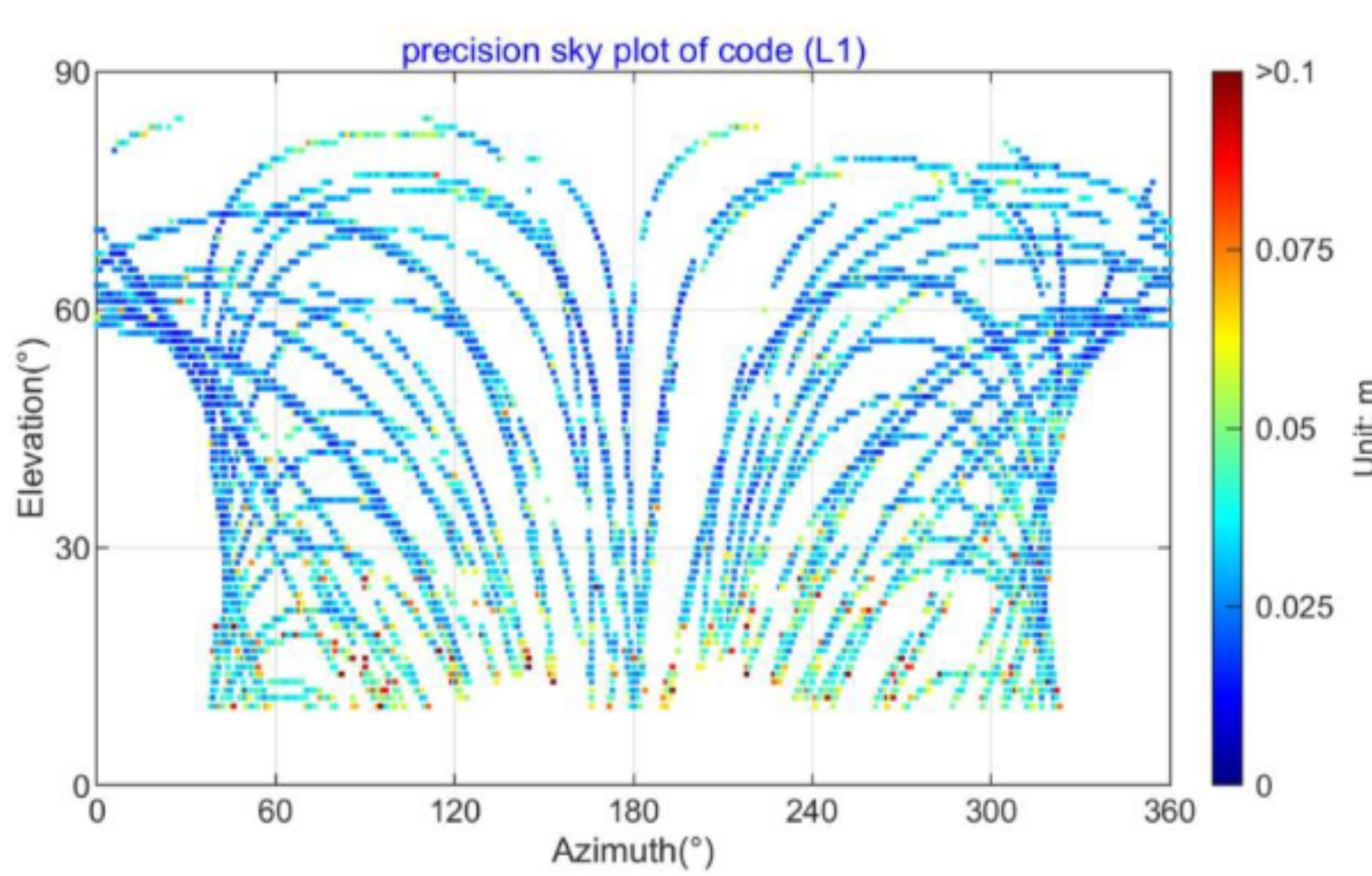


**Fig. 30** 2D plane plot of code PMHM for GPS

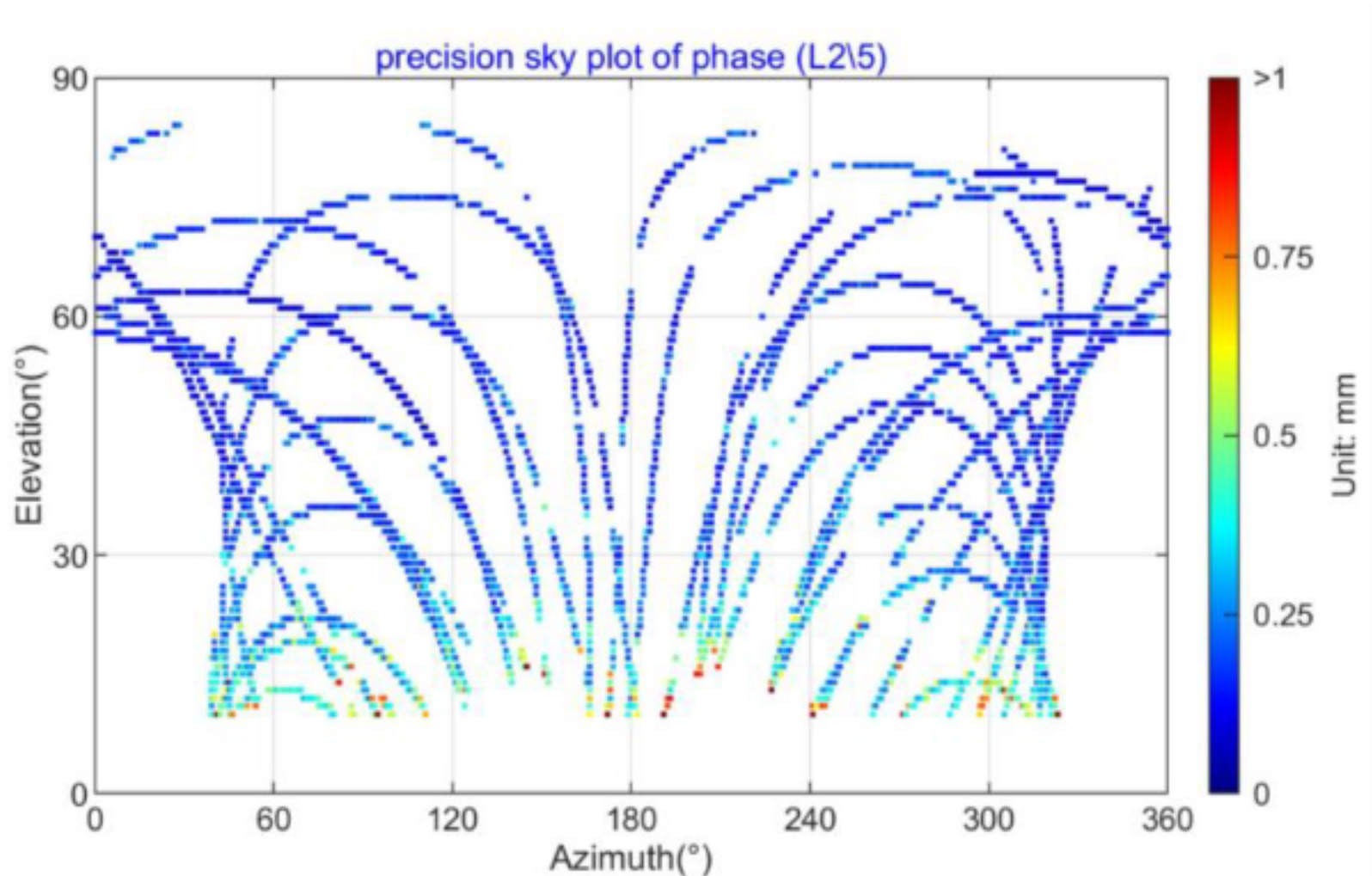


**Fig. 31** 2D plane plot of phase PMHM for GPS

### 3. SMHM

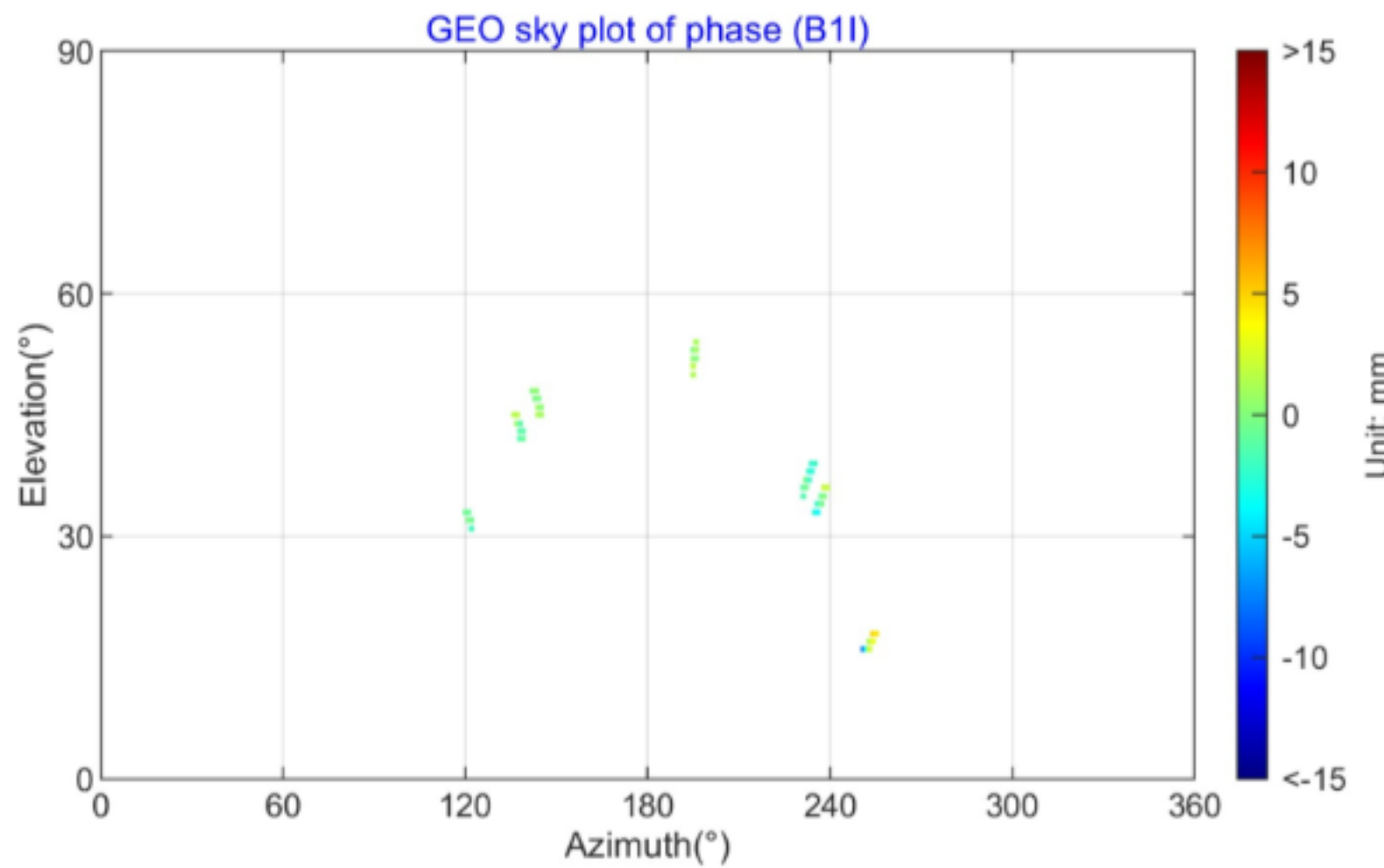


**Fig. 32** 2D plane plot of phase SMHM for BDS GEO satellites

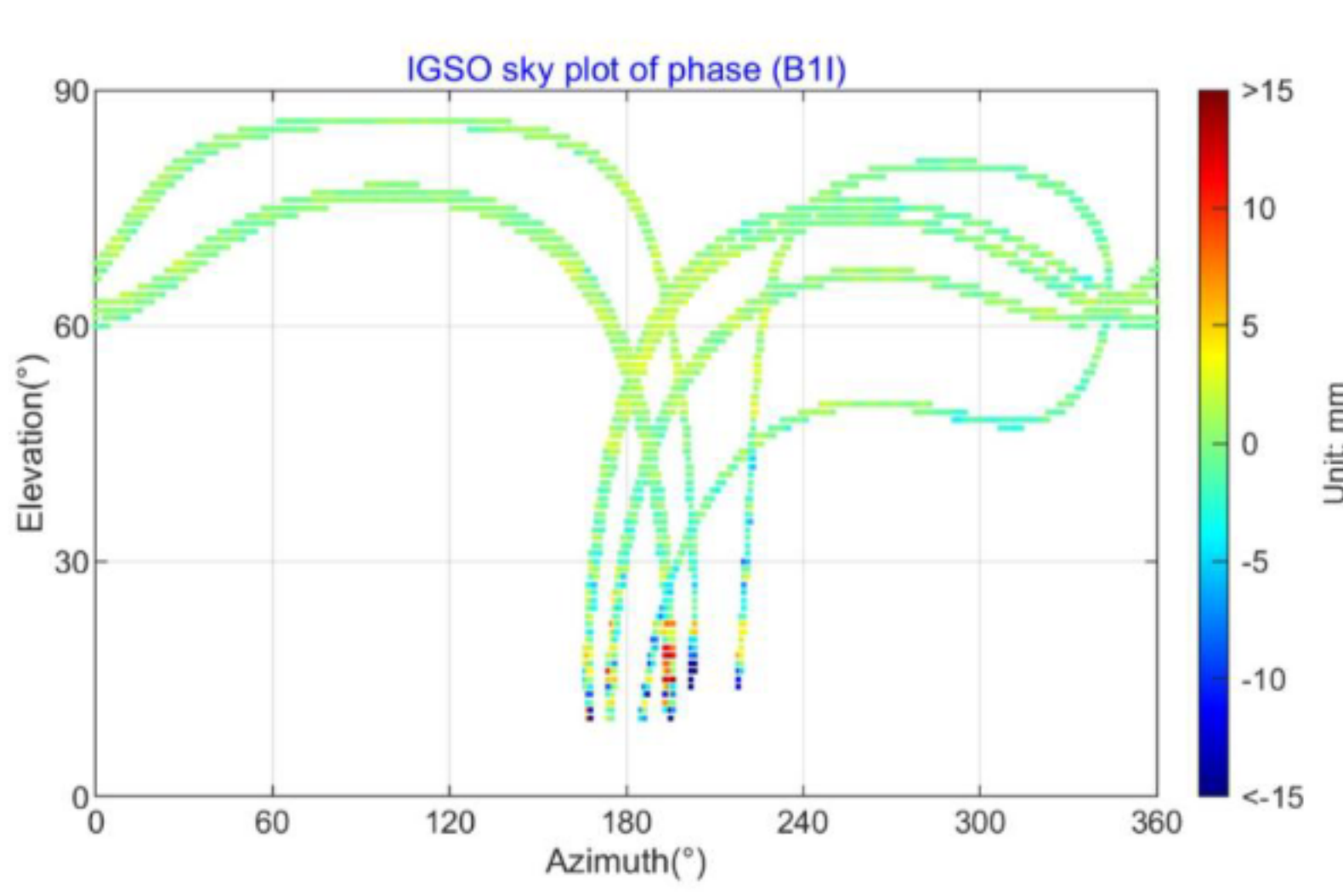


**Fig. 33** 2D plane plot of phase SMHM for BDS IGSO satellites

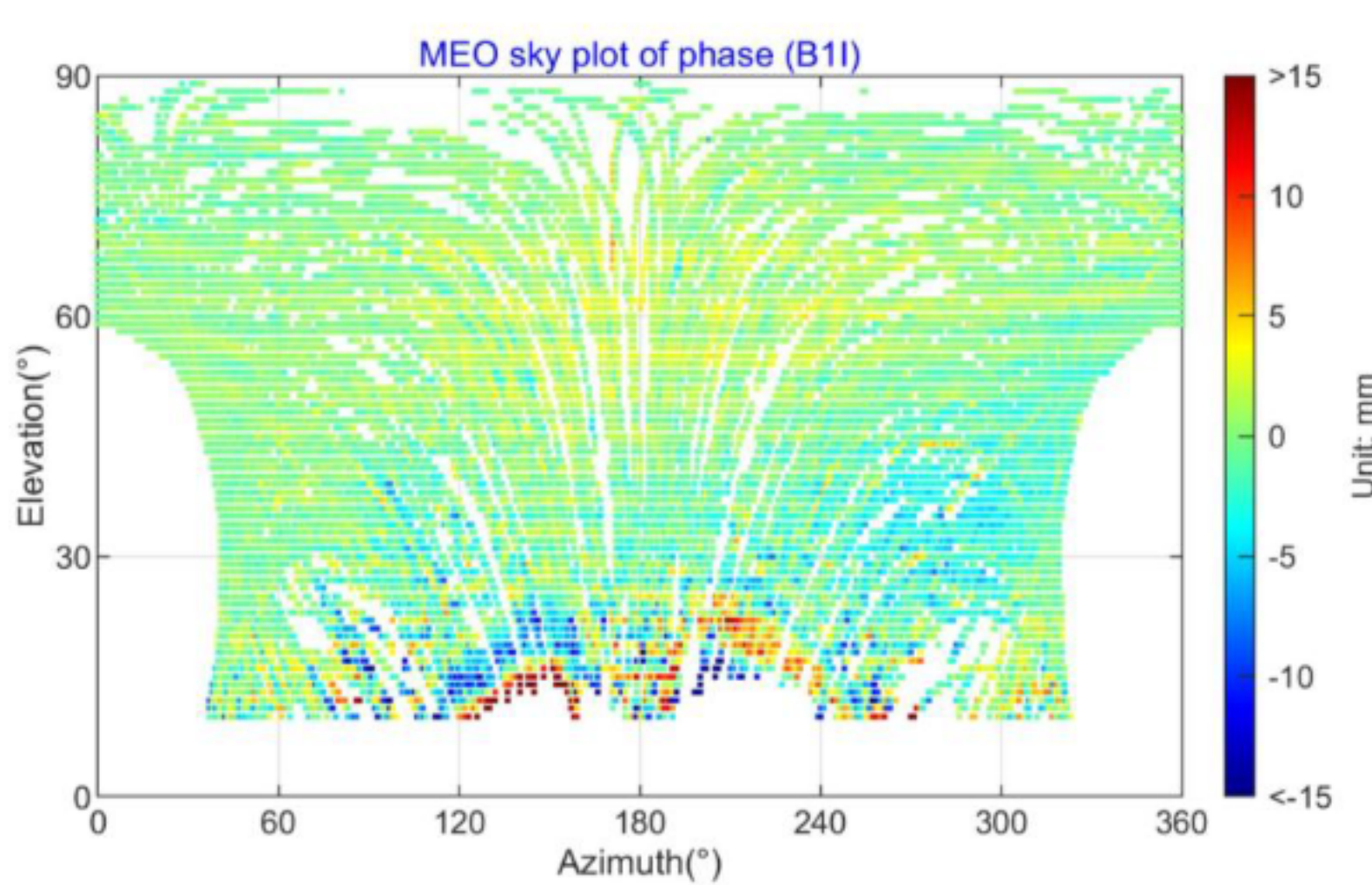


**Fig. 34** 2D plane plot of phase SMHM for BDS MEO satellites

### 4. FMHM

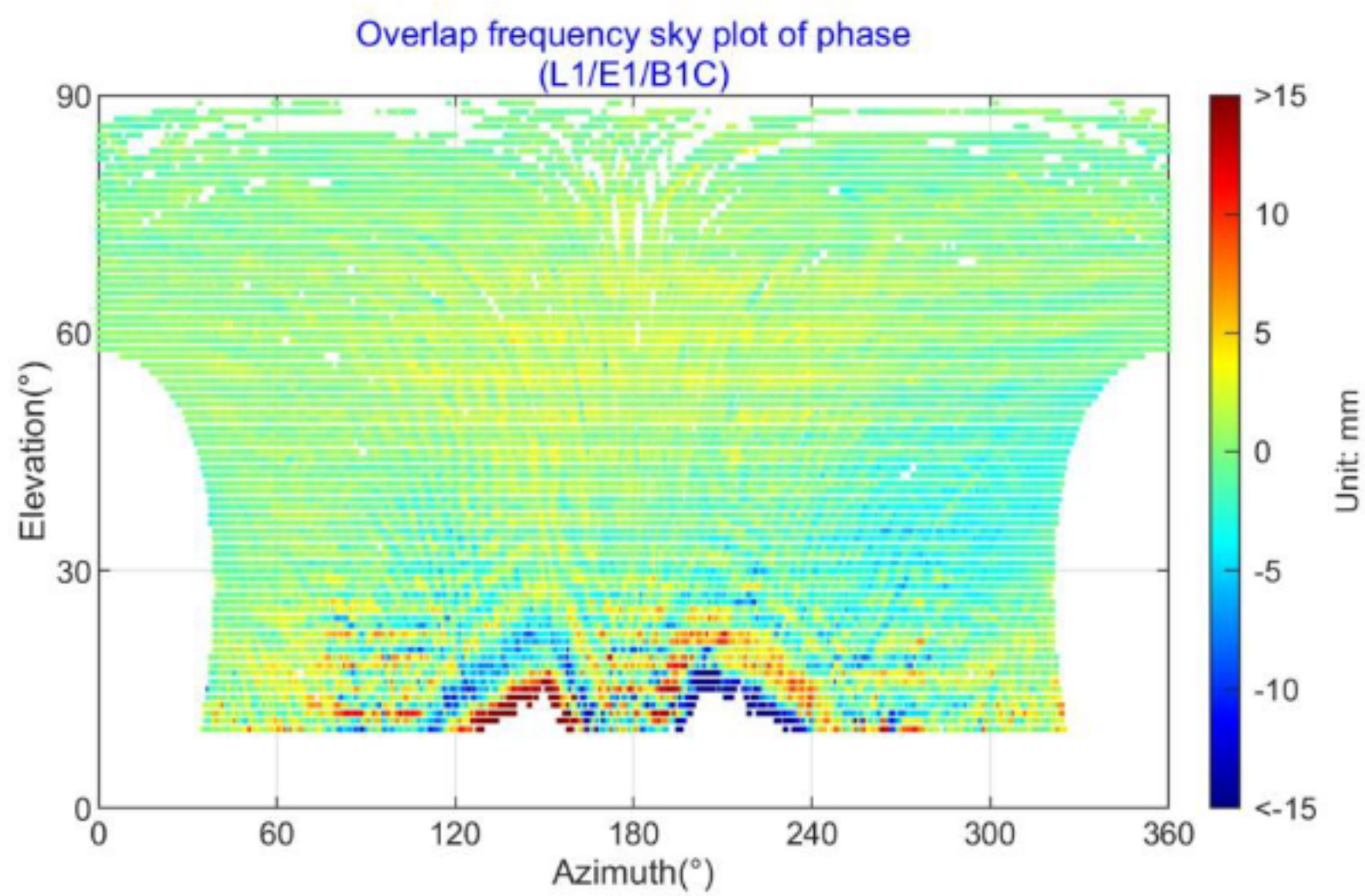


**Fig. 35** 2D plane plot of phase FMHM for L1/E1/B1C

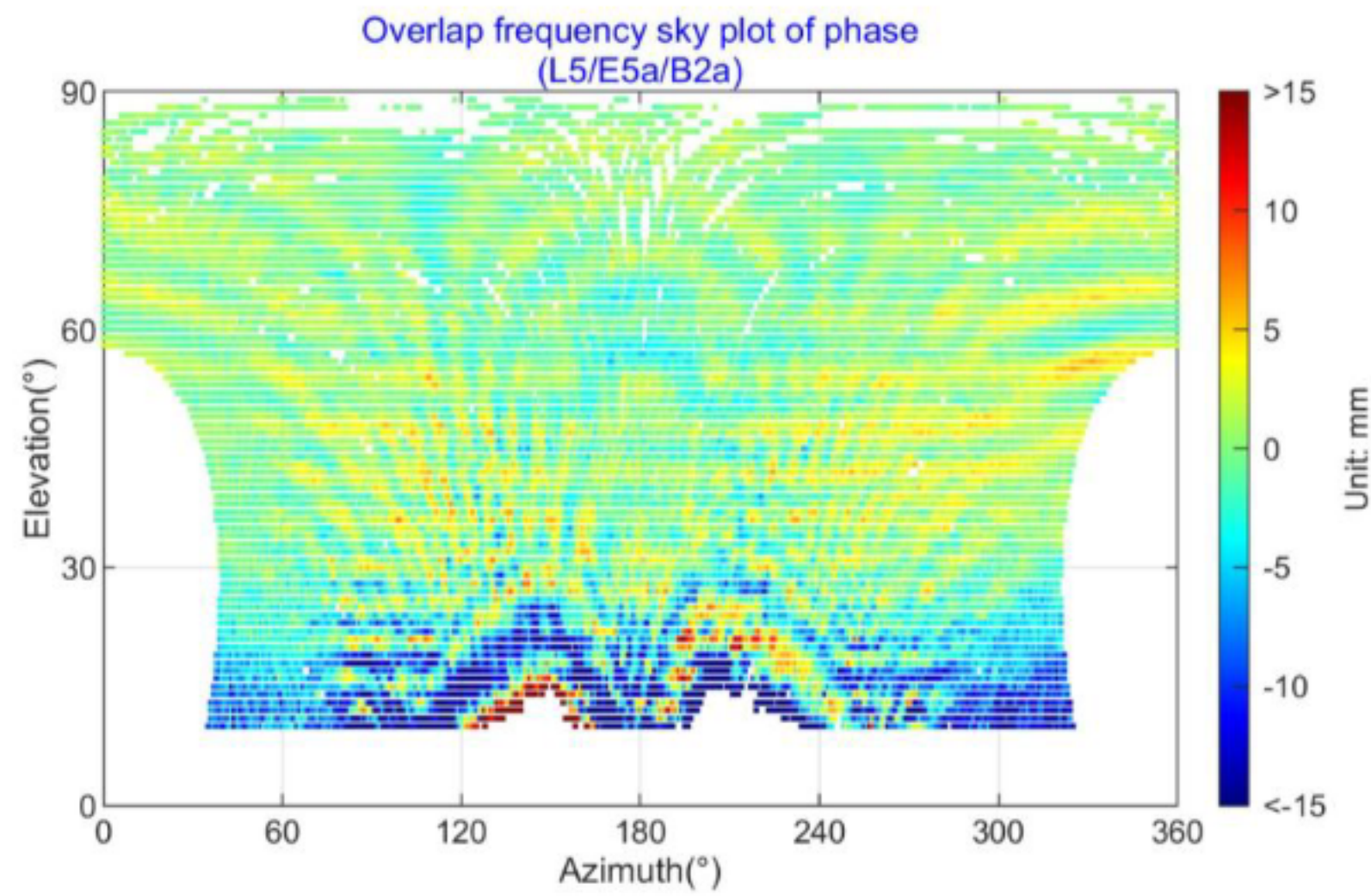


**Fig. 36** 2D plane plot of phase FMHM for L5/E5a/B2a

### 5.2.3 3D sky plot

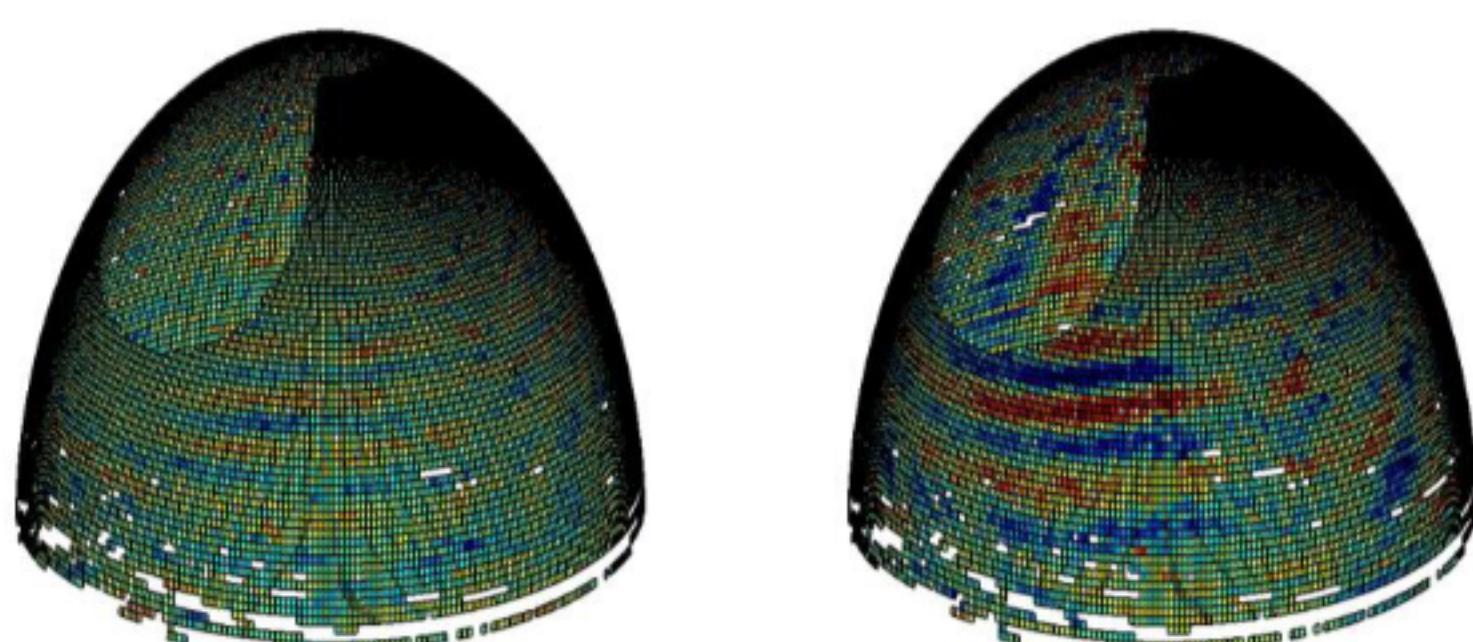
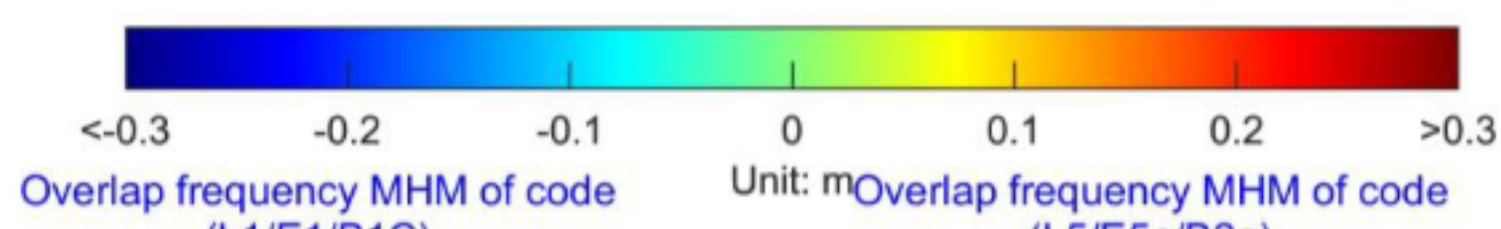


**Fig. 37** 3D sky plot of code FMHM

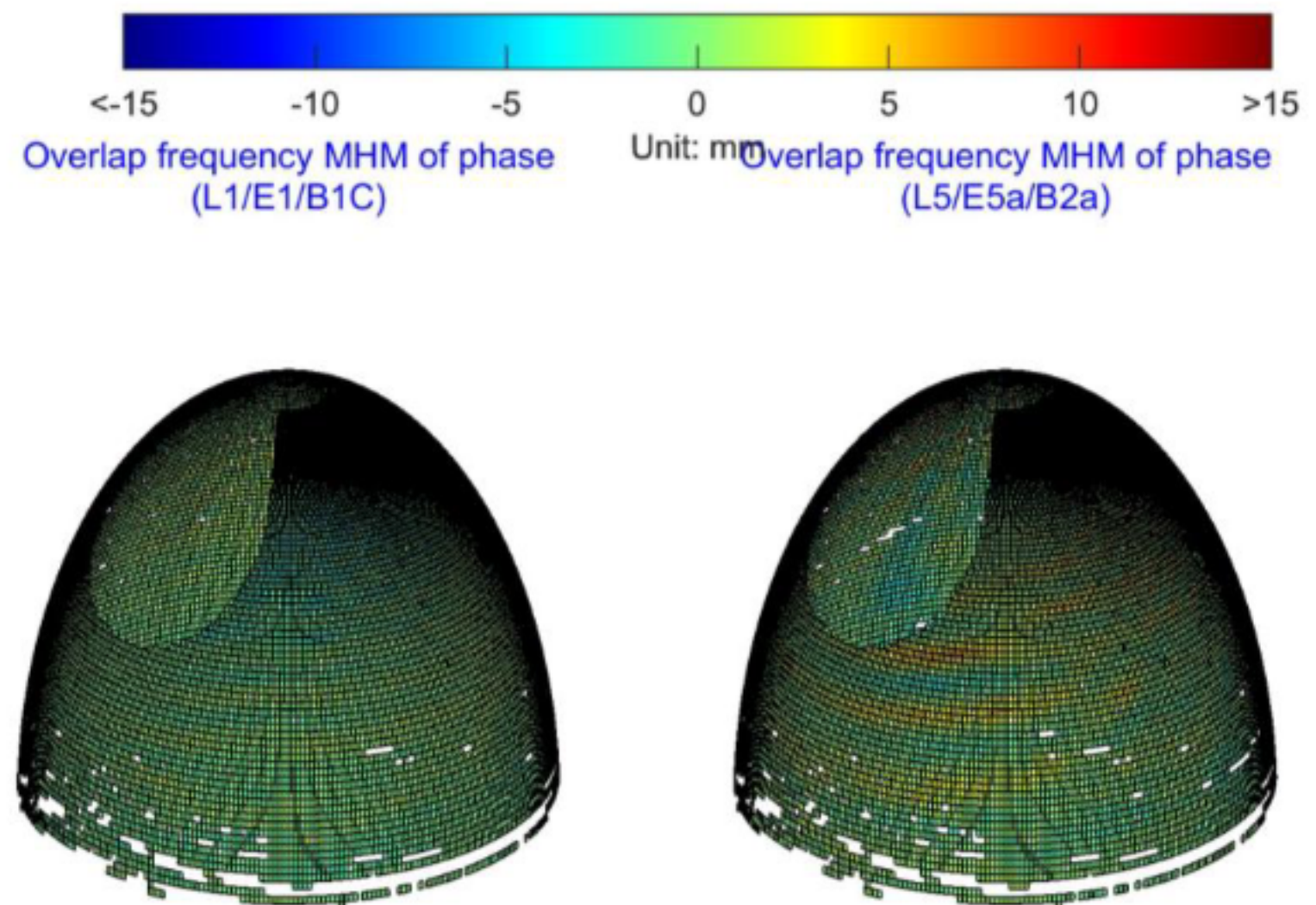


**Fig. 38** 3D sky plot of phase FMHM

### 5.3 Plotting of SF modeling

For the SF modeling part, the plotting of SF and SF\_W models are supported. Some typical results are shown as following.

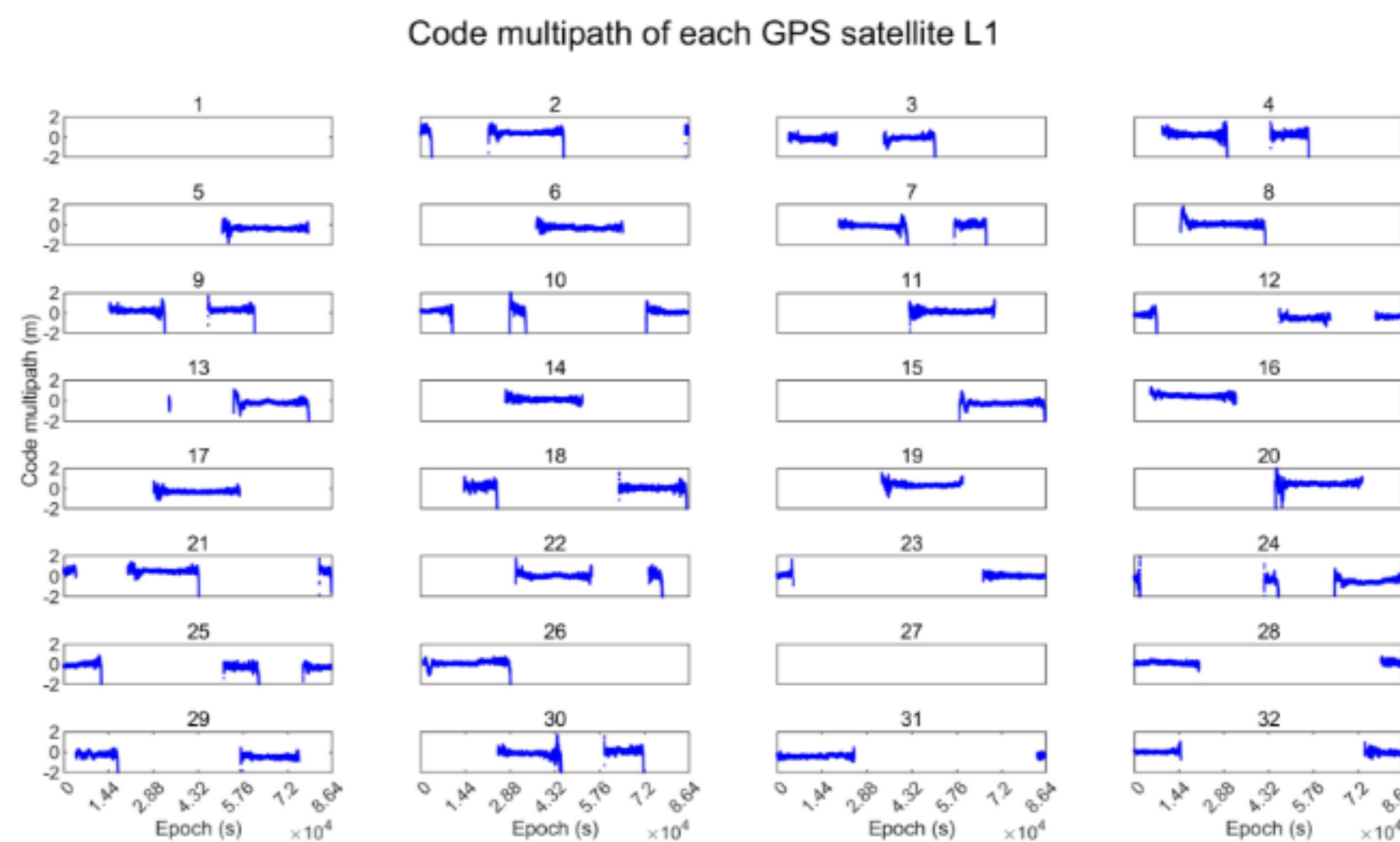


**Fig. 39** Time series plot of SF GPS L1 code multipath using SF model

Code multipath of each GPS satellite L1

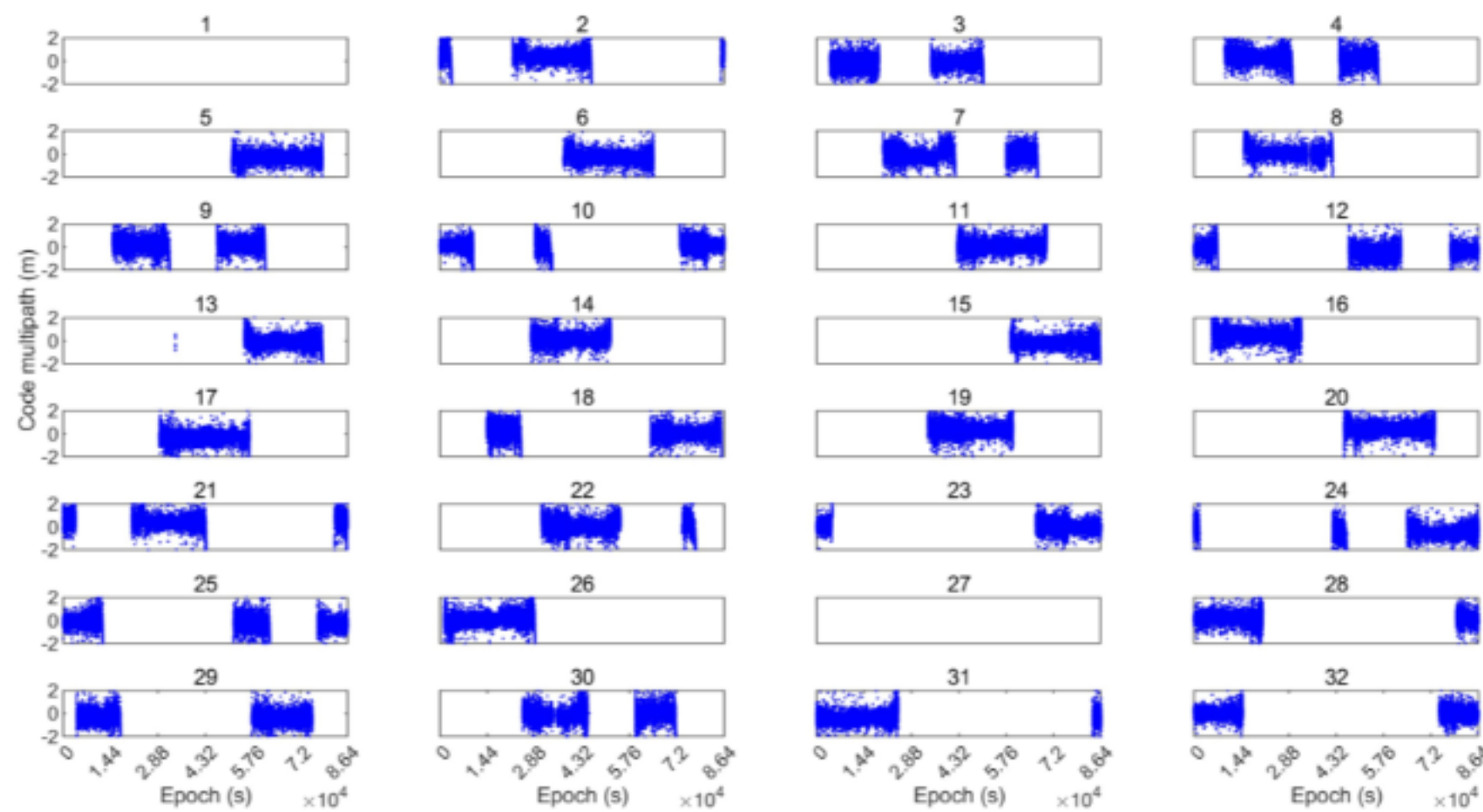


**Fig. 40** Time series plot of SF GPS L1 code multipath using SF\_W model

Code multipath of each GAL satellite E1

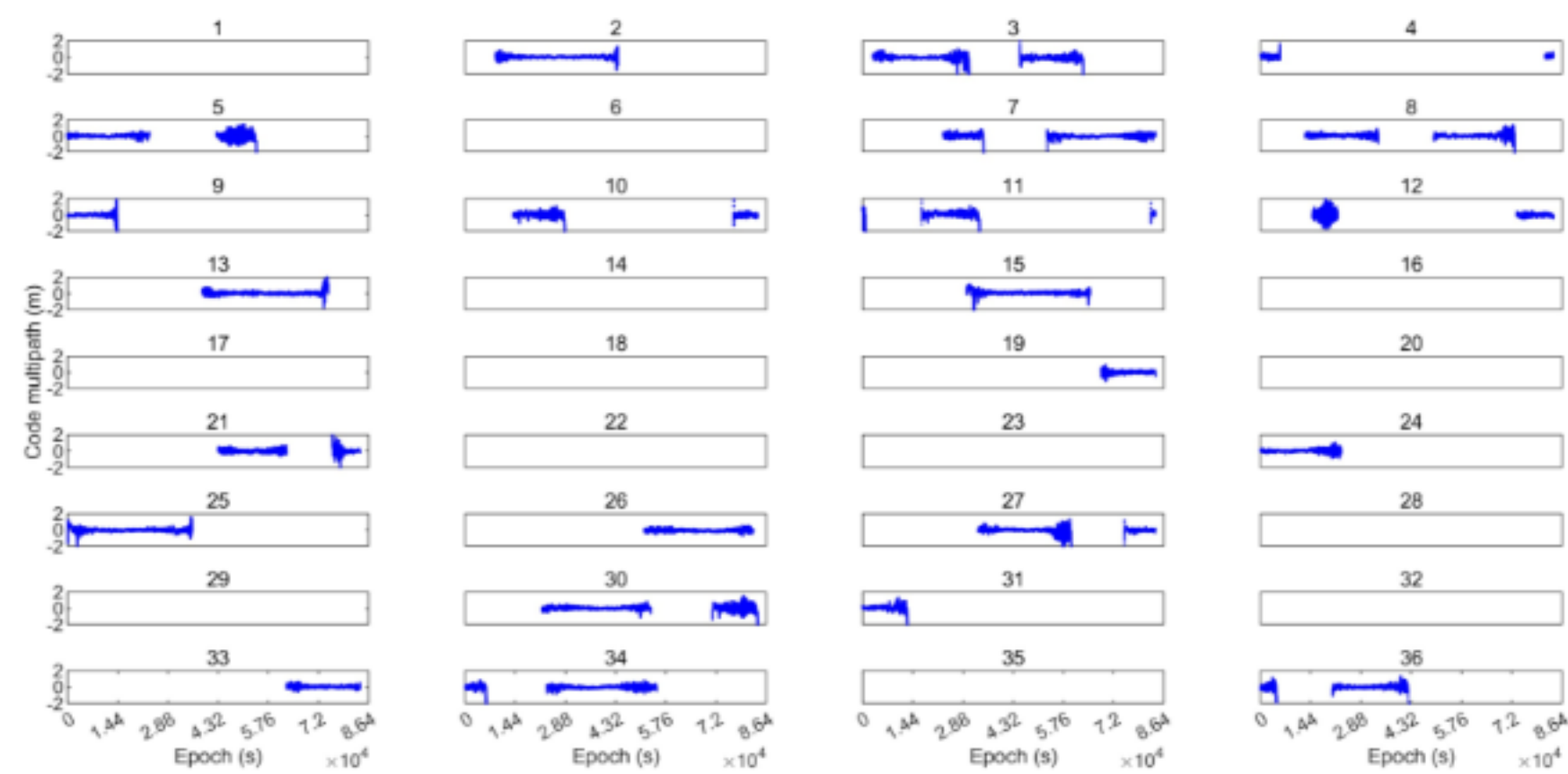


**Fig. 41** Time series plot of Galileo E1 code multipath using SF model

Code multipath of each GAL satellite E1

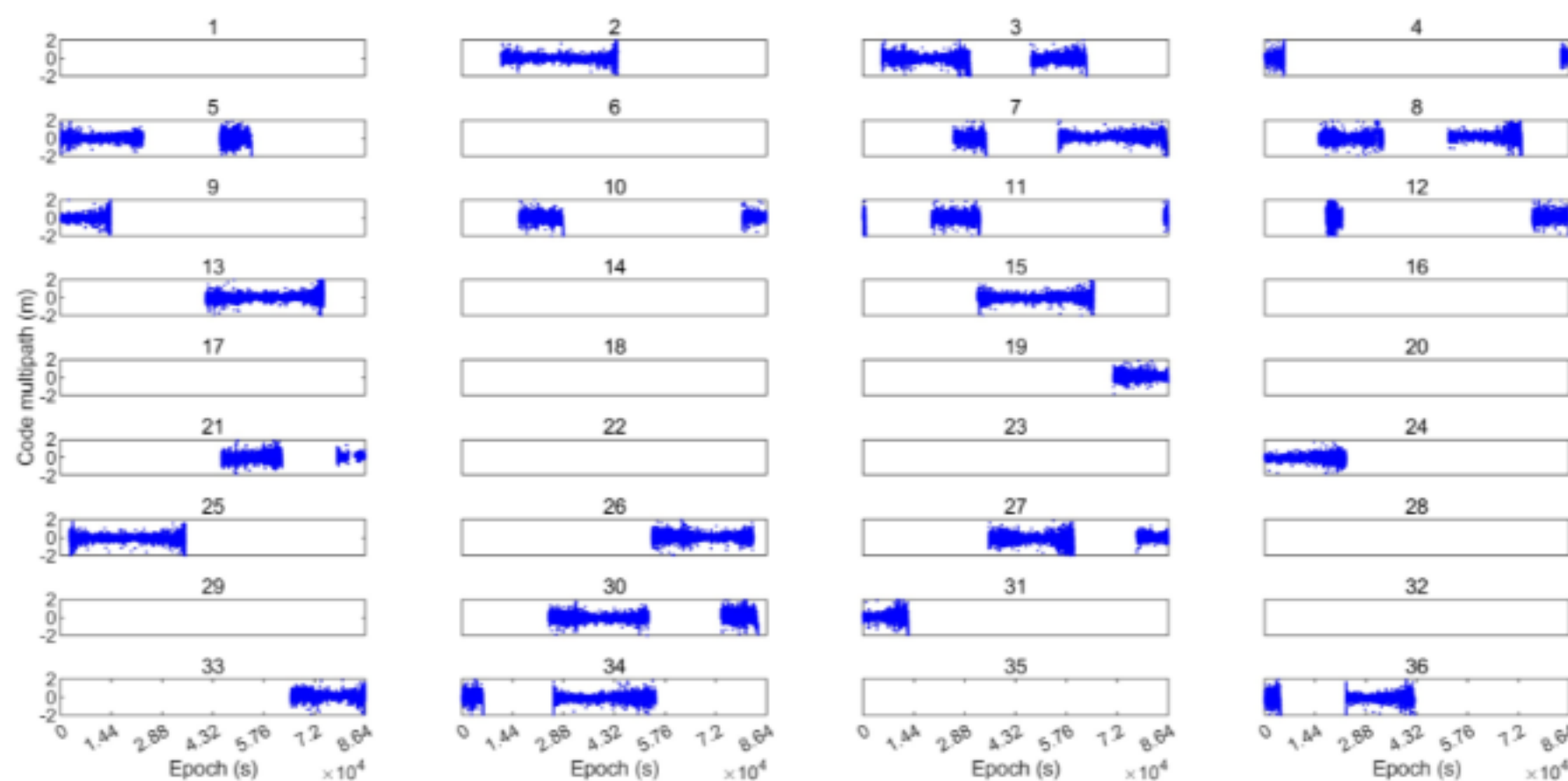


**Fig. 42** Time series plot of Galileo E1 code multipath using SF\_W model

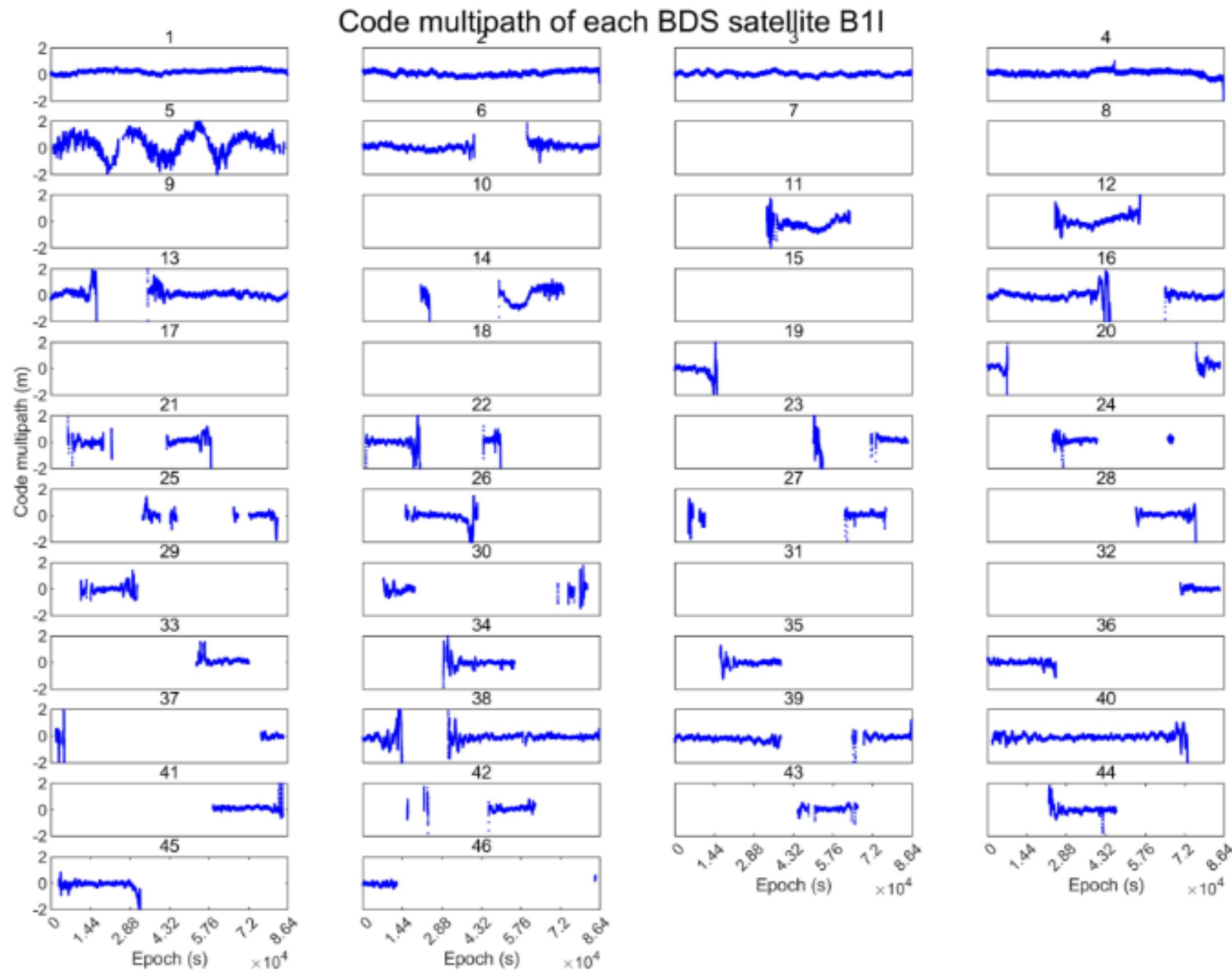


**Fig. 43** Time series plot of BDS B1I code multipath using SF model

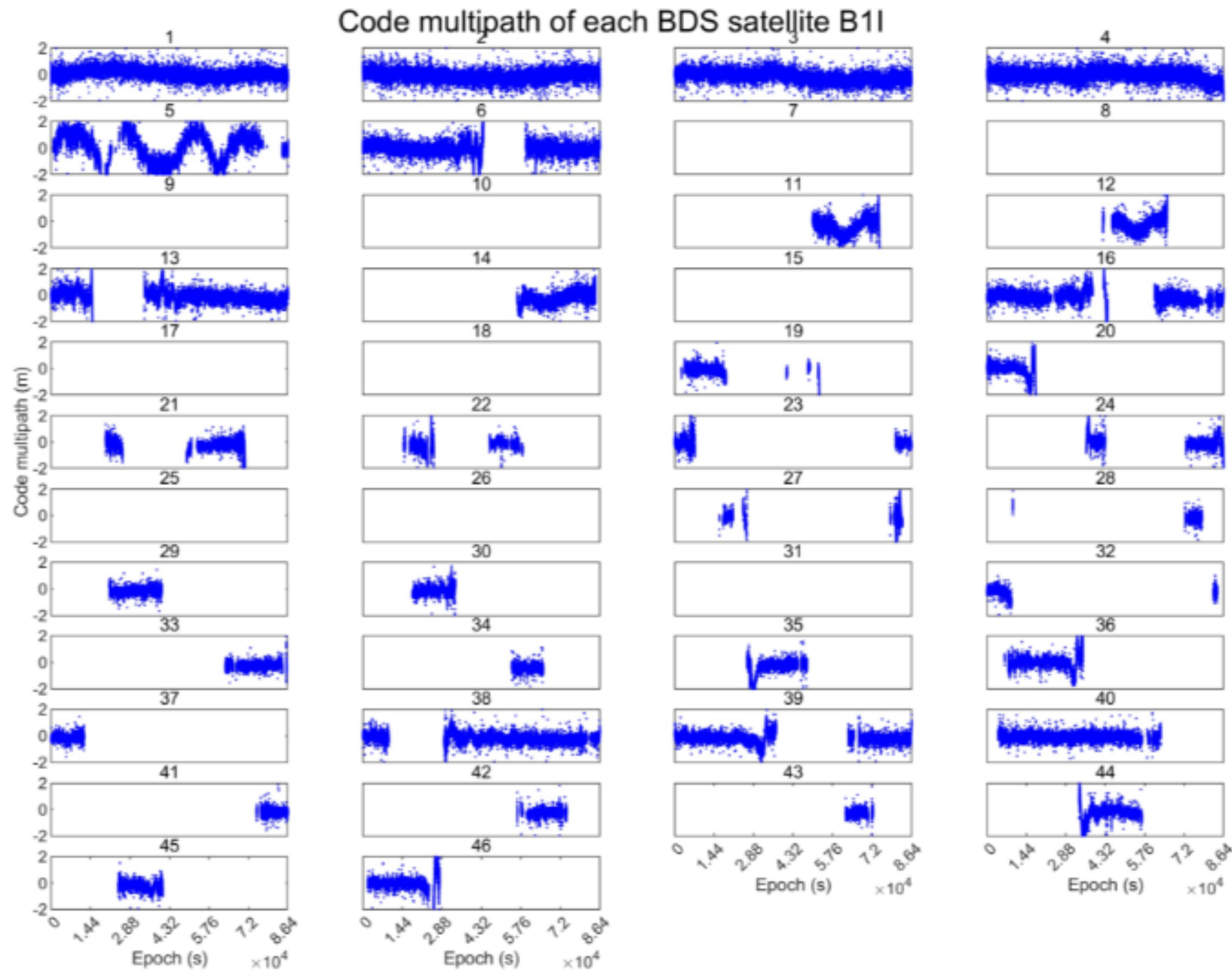


**Fig. 44** Time series plot of BDS B1I code multipath using SF\_W model

## 6 Acknowledgement

The MAPS is developed based on MATLAB R2021a, and we are grateful to the MATLAB developers for their works. Part of the code of the MAPS is based on raPPPid software, and we are grateful to Glaner, MF, and Weber, R for their work. We are grateful to the RTKLIB software, on which our residual files are generated. In addition,

we would like to thank the IGS and MGEX organizations, such as CODE, CAS, and WHU, for providing GNSS observations and related products.

## 7 Disclaimer

The experiment is carried out in MATLAB 2021a environment. With the update of the software, proper modifications of the code may be needed. Some bugs may still exist in the MAPS, comments and suggestions are welcome to send to the authors.

## 8 Contact us

GCC research group of dedicated developers earnestly seeks your valuable insights and suggestions to improve the MAPS. We welcome all users to share and exchange technical details, as well as provide improvement suggestions. Here are our contact details:

GitHub: <https://github.com/GCCProTeam>

Emails: zt.zhang@hotmail.com; navyyuan@yeah.net

## Reference

- Anscombe FJ (1973) Graphs in statistical analysis. *Am Stat* 27(1):17-21.
- Bock Y, Nikolaidis R, Jonge P, Bevis M (2000) Instantaneous geodetic positioning at medium distances with the global positioning system. *J Geophys Res Solid Earth* 105(B12):28223-28253.
- Chayes F (1970) On deciding whether trend surfaces of progressively higher order are meaningful. *Geol Soc Am Bull* 81(4):1273-1278.
- Cornell JA (1987) Factors that influence the value of the coefficient of determination in simple linear and nonlinear regression models. *Phytopathology* 77(1):63-70.
- Glaner MF, Weber R (2023) An open-source software package for Precise Point Positioning: raPPPid. *GPS Solut* 27 (174).
- Glaner MF (2022) Towards instantaneous PPP convergence using multiple GNSS signals. Technische Universität Wien, Vienna.
- Koch K (1999) Parameter estimation and hypothesis testing in linear models. Springer, Berlin.
- Lehmann E, Romano J (2006) Testing statistical hypotheses. Springer, Berlin.
- Leick A, Rapoport L, Tatarnikov D (2015) GPS satellite surveying. Wiley, New York.
- Lu R, Chen W, Dong D, Wang Z, Zhang C, Peng Y, Yu C (2021) Multipath mitigation in GNSS precise point positioning based on trend-surface analysis and multipath hemispherical map. *GPS Solut* 25(3):119.
- Ragheb AE, Clarke PJ, Edwards SJ (2007) GPS sidereal filtering: coordinate- and carrier-phase- level strategies. *J Geod* 81(5):325–335.
- Shen N, Chen L, Wang L, Lu X, Tao T, Yan J, Chen R (2020) Site-specific real-time GPS multipath mitigation based on coordinate time series window matching. *GPS Solut* 24:82.
- Sobol MG (1991) Validation strategies for multiple regression analysis: using the coefficient of determination. *Interfaces* 21:106–120

- Strode P, Groves P (2015) GNSS multipath detection using three-frequency signal-to-noise measurements. *GPS Solut* 20(3):399-412.
- Wang Z, Chen W, Dong D, Wang M, Cai M, Yu C, Zheng Z, Liu M (2019) Multipath mitigation based on trend surface analysis applied to dual-antenna receiver with common clock. *GPS Solut* 23:104.
- Yuan H, Zhang Z, He X, Zeng J, Wang H (2024) Improved Multipath Mitigation Using Multiple Trend-Surface Hemispherical Map in GNSS Precise Point Positioning. *IEEE Sens. J* 24(8):13095-13103.
- Zhang Z, Dong Y, Wen Y, Luo Y (2023) Modeling, refinement and evaluation of multipath mitigation based on the hemispherical map in BDS2/BDS3 relative precise positioning. *Measurement* 213.
- Zhang Z, Dong Y, Wen Y, Yuan H, Li B (2024) Robust Pseudorange and Carrier Phase Multipath Mitigation With Hemispherical Map Considering the Uncertainty. *IEEE Sens. J* 24(7):10832-10840.
- Zhang Z, Li B, Gao Y, Shen Y (2019) Real-time carrier phase multipath detection based on dual-frequencyC/N0 data. *GPS solut* 23:7.
- Zhang Z, Yuan H, Li B, He X, Gao S (2021) Feasibility of easy-to-implement methods to analyze systematic errors of multipath, differential code bias, and inter-system bias for low-cost receivers. *GPS Solut* 25:116.